NOAA Technical Memorandum ERL ESG-4

VARIABILITY OF THE CONVECTIVE FIELD PATTERN IN SOUTH FLORIDA AND ITS RELATIONSHIP TO THE SYNOPTIC FLOW

Environmental Sciences Group
Boulder, Colorado
January 1984

noaa NATIONAL OCEANIC AND ATMOSPHERIC ADMINISTRATION / Environmental Research Laboratories

NOAA Technical Memorandum ERL ESG-4

VARIABILITY OF THE CONVECTIVE FIELD PATTERN IN SOUTH FLORIDA AND ITS RELATIONSHIP TO THE SYNOPTIC FLOW

David O. Blanchard
Raúl E. López

Weather Research Program

Environmental Sciences Group
Boulder, Colorado
January 1984

UNITED STATES
DEPARTMENT OF COMMERCE

Malcolm Baldrige,
Secretary

NATIONAL OCEANIC AND
ATMOSPHERIC ADMINISTRATION

John V. Byrne,
Administrator

Environmental Research
Laboratories

Vernon E. Derr,
Director

NOTICE

Mention of a commercial company or product does not constitute an endorsement by NOAA Environmental Research Laboratories. Use for publicity or advertising purposes of information from this publication concerning proprietary products or the tests of such products is not authorized.

CONTENTS

FIGURES

FIGURE PAGE

TABLES

VARIABILITY OF THE CONVECTIVE FIELD PATTERN IN SOUTH FLORIDA AND ITS RELATIONSHIP TO THE SYNOPTIC FLOW

David O. Blanchard and Raúl E. López

ABSTRACT. Although they are a fairly consistent feature, the sea-breeze and lake-breeze convergence lines and the associated convection over south Florida during the summer may vary considerably from day-to-day. An examination of the daily convective patterns indicates that there are a few basic recurring patterns. Analyses of radiosonde data show significant differences in the local thermodynamic parameters, most notably the specific humidity. Changes in the synoptic scale wind field correspond closely to changes in the observed convective patterns and the local thermodynamic conditions. Explanation of the formation and development of the different patterns of convection are given in terms of the complex interaction between the regional-, synoptic-, peninsular- and local- scale circulations.

1. INTRODUCTION

The most consistent convective features over south Florida in the summer are the sea- and lake-breeze lines. In fact, some people claim to be able to set their watches by the development and onset of thundershowers associated with the sea-breeze convergence zones. Observations and data, however, indicate that the situation is less reliable than this simple assumption since variations of convective activity can be large in both space and time in south Florida. In particular, rainfall amounts and echo area coverage can both vary by up to an order of magnitude from one day to the next.

It is these day-to-day variations that can prove both interesting and occasionally frustrating for the forecaster in south Florida, who must determine when and where convection will occur on a daily basis. The forecaster's primary guidance lies in the synoptic-scale flow patterns, and the problem becomes one of determining in an objective way how these different large-scale patterns interact with the peninsular and local scale thermal circulations (i.e., sea breezes, lake breezes, etc.) and surface

features to produce large variations in the timing and spatial distribution of convective developments.

The goal of this study is to investigate the principal factors determining the spatial and temporal variations of the convective field in south Florida during the summer, and to quantify these factors in order to provide a useful tool for the forecaster.

It is expected that under certain synoptic regimes, distinct temporal and spatial patterns of convection will develop. The timing, intensity, and motion of the sea- and lake-breeze convergence zones and their attendant convection, for example, are possibly dependent to a large degree on the synoptic-scale flow. Surface features such as Lake Okeechobee, the water conservation areas, and the coastal configuration also play varying roles in the generation, maintenance, and decay of circulations on the peninsular and local scales, which in combination with the large scale flow, may provide the necessary mechanisms to account for nearly all of the observed large day-to-day variability under synoptically undisturbed conditions.

In order to determine the possible relationships between the synoptic- and peninsular-scale flows in combination with the surface features and the resulting temporal and spatial distributions of convection, it was decided to ascertain if there were recurrent patterns in the organization of the convective field and then try to determine what meteorological conditions and surface features were associated with them.

The convective field was examined using radar data collected in 1975 and 1978 during the Florida Area Cumulus Experiment (FACE). Inspection of three-hour averages of radar echo intensity and composites of areal coverage for each of the days resulted in the determination of several typical patterns. Individual days were then grouped into one of several types, according to the convective pattern prevalent on that day. The regional- and synoptic-scale flow and moisture characteristics corresponding to each of the different types were studied using wind field maps for constant pressure surfaces and

the boundary layer, surface pressure charts, and atmospheric soundings. Finally, an empirical model was developed to explain the formation and evolution of the different patterns in terms of the complex interaction between the regional-, synoptic-, peninsular- and local-scale flows.

Spatial and temporal organization of the convective field in south Florida has been noted by other investigators in the past. Results of both observational and numerical modeling studies have pointed to the existence of a number of patterns that are linked, in part, to the regional- and synoptic-scale flow. Byers and Rodebush (1948) were the first to recognize the importance of the sea breeze as a forcing mechanism for convection in central and south Florida. In addition, they suggested that the large-scale circulation may have an important influence on Florida rainfall. Day (1953) noted that the air mass over Florida during the summer is almost always identifiable as maritime, but that the southeast coast of Florida has periods without precipitation while the interior portions of the peninsula remain convectively active. He attempted to explain these patterns using divergence profiles obtained with the Bellamy (1949) nomograph method, but was unable to reach any conclusions because of an inadequate data set. Later, Gentry and Moore (1954), using wind and raingage data from the Miami area, were able to conclude that the organized patterns were controlled by the areas of convergence created by the interaction of the general (synoptic-scale) wind and local winds. They were able to determine the differences in general winds responsible for the "afternoon" and "night and morning" types of convection. This interaction between the sea breeze and the prevailing wind pattern was also observed by Riehl (1954) on the island of Puerto Rico.

No further observational work was done until Frank et al. (1967) published an important paper relating convective patterns to different flow regimes. Radar data from Daytona Beach, Tampa, and Miami in Florida were manually digitized for three summers. The data were stratified by wind direction using 1524 m (5000 ft) winds. Maps depicting the frequency of occurrence of radar echoes were obtained for each of five

wind types: northerly, easterly, southerly, and westerly winds, all greater than 3 ms^{-1}, and light and variable winds. The results show the strong influence exerted on convection by the sea and lake breezes, in addition to both larger and smaller scale influences. Their data, however, were limited in the sense that radar echoes were recorded only once every 3 hours, and no echo intensity information was recorded.

Later, Frank and Smith (1968) attempted to correlate the percentage of the study area in Florida covered by radar echo at specified times with numerous synoptic parameters, including humidity, divergence, vorticity, temperature, and height of many pressure levels. Their results indicate that mid-tropospheric (750 mb and 650 mb) humidity was the most highly correlated, having correlation coefficients of .60 and .65, respectively. All other parameters showed little or no relationship with areal coverage.

Smith (1970) performed a study similar to that of Frank et al. (1967) using radar data and winds from Apalachicola, Florida. His results indicated that the "concave/convex coastline effect" played a major role in the formation and location of echoes. This was in agreement with McPherson's (1970) numerical model which showed that the presence of a bay or other large indentation of a coastline produced a landward distortion of the sea-breeze convergence zone which is damped out with time.

Pielke (1973), in an observational study, determined that the convective field patterns are best defined on days with a small time variation in the deep layer mean winds and a small difference in the mean wind between Miami and Tampa. Additionally, initial echo formation had a tendency to occur in geographically favored regions; in particular, the area east of Lake Okeechobee appeared to have a maximum of echo coverage for several different wind directions. No obvious correlation was noted between the (subjective) degree of organization and the low vertical wind shear or mean mixing ratio in the the lower troposphere. Results from this study were used as part of the verification for Pielke's (1974) three-dimensional numerical mesoscale model. He noted that on days without significant organized synoptic-scale disturbances overlying

south Florida, the sea-breeze convergence patterns were the primary control of the general locations of the cloud and shower complexes. The sea-breeze convergence zones, and their movement with time, in turn, were controlled by the large scale flow. The effects of Lake Okeechobee were also tested with the model. Experiments were conducted that included and excluded the lake, and the results were compared. The model indicated that Lake Okeechobee produced a lake breeze circulation, which reinforced the convergence caused by the larger scale sea breeze. These model results agreed well with results from the previous observational study.

In a subsequent refinement and verification of the model, Pielke and Mahrer (1978) noted that although most of the showers occurred in the predicted convergence zones, much of the convergence region was not covered by precipitating clouds, indicating that sea-breeze convergence was a necessary, but not sufficient, condition for most of the convection that occurs on synoptically undisturbed days. Later, Gannon (1978) and McCumber (1980) updated Pielke's model to include soil types and moisture, vegetation, and the variation of incoming solar radiation due to clouds. They found that all of these factors played significant roles in the determination of the location and intensity of the convergence zones generated by the sea breeze. Also, Gannon's (1978) model consistently verified Estoque's (1962) early sea-breeze model results, showing the sensitivity of the sea-breeze intensity, extent, and shape to the prevailing geostrophic flow.

Thus, in the past 35 years, considerable progress has been made contributing to the understanding of convection in south Florida during the summer. Observational studies and numerical model results have all indicated that there is a strong relationship between convection and the sea-breeze and large-scale flow. Additionally, surface characteristics can play an important role in this complex interaction of scales.

The radar data set used in the present study far exceeds previous data sets in both spatial and temporal resolution, and also includes information on echo intensity. It is

believed that by using these higher resolution data, additional information regarding the complex interrelationships between the many interacting scales (synoptic, peninsular, local) can be obtained and will contribute to a better understanding of the dynamics and kinematics of the synoptic-scale flow, the sea breezes, and cumulus convection of south Florida.

2. DATA SOURCES AND PROCESSING TECHNIQUES

2.1. The Florida Area Cumulus Experiment

The data used in this study were collected in conjunction with the first phase of the Florida Area Cumulus Experiment (FACE) during the summer months of 1975 and during the second phase of FACE during the summer months of 1978. The principal objective of the experiment was to confirm the hypothesis that rainfall was increased over a large area (1.3×10^4 km^2) by selectively treating active cumulus clouds with silver iodide (Woodley et al., 1982). The area over which the experiment was conducted is indicated by the shaded quadrilateral in Fig. 1. This area is referred to as the Target Area (TA). A detailed description of the FACE-1 and FACE-2 operations and data inventory can be found in Cumulus Group Staff (1976, 1979). The experiment ran from June 15 to September 15 in 1975 and from June 15 to August 31 in 1978; however, only data from the period July 1 to August 31 for both years were used in this study. Data were collected on 114 days out of a possible 124 days. A WSR-57 radar was located in the city of Coral Gables, southwest of Miami, and scanned the area continuously during the hours when the experiment was carried out (usually from 0900 to 2100 EDT) except for downtime. Data were collected for a full 360° scan from 29.6 km (16 nmi) to 214.6 km (116 nmi) covering an area of 1.4×10^5 km^2. Clouds were treated with inert sand or silver iodide on 37 days (20 with inert sand and 17 with silver iodide) of the period mentioned above as part of the randomized seeding experiment. These days were selected on the basis of an estimated growth potential for the clouds of that day in the event of their being seeded with silver iodide. Radar data, however, were collected for all days. The data used in this study came from all possible days, including both treated

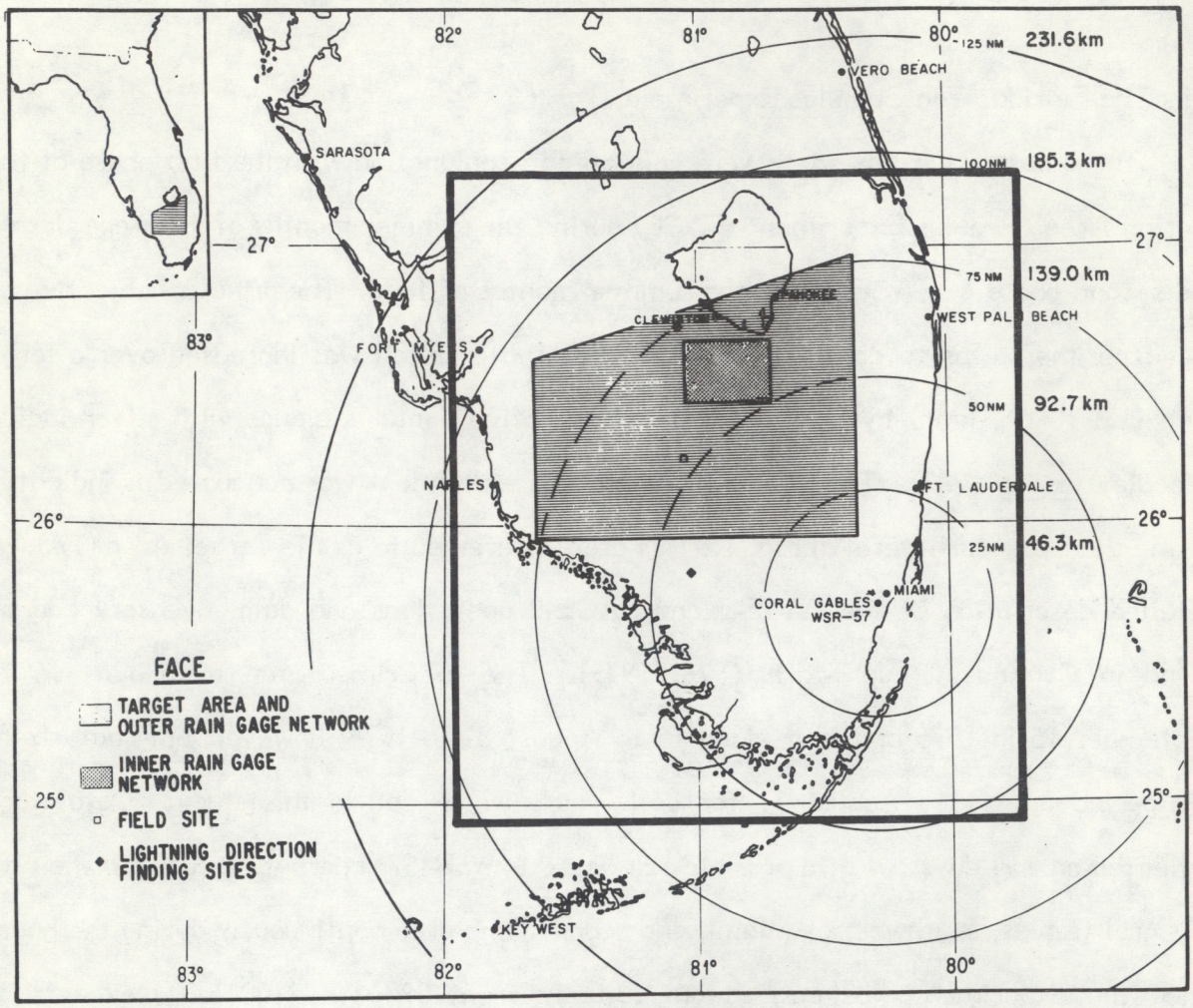

Figure 1. Map of south Florida showing the FACE target area, the position of the WSR-57 radar and the range mark from the radar. The heavy outline indicates the subarea for which radar data are presented.

and untreated days. No stratification by treatment was considered in this paper since the TA is less than 10% of the total study area and, additionally, on any given day, the ratio of treated cell area to total cell area of the TA is far less than unity. Thus, any effect that treatment may have on the convective cloud field in the TA should be insignificant when considered over the much larger scale used in this study.

2.2. Radar Data

The radar data used were obtained with a WSR-57 radar system belonging to the National Hurricane Center, a part of the National Weather Service. A detailed description of this radar and of the collection and processing schemes used can be found in Lopez et al. (1981). The WSR-57 is an S-band radar (wavelength of 10.53 cm) having a circular antenna that produces a vertical and horizontal halfpower beamwidth of 2.2°. The minimum detectable signal (MDS) of the radar is set to -103 dBm.

The antenna was rotated constantly at 3 rpm and was aimed at an elevation of 0.5 degrees. The WSR-57 radar was operated continuously 24 hours per day by National Weather Service personnel, and the radar digitizer was operated continuously from 0900 to 2100 EDT during all the days of the 1975 and 1978 field programs by FACE personnel. The data were digitized and recorded on magnetic tapes (see Wiggert and Andrews (1974) for a complete description of this process). The returned power signal of the radar was nominally integrated for sectors of 930 m (0.5 nmi) in range and 2° of azimuth. The data were digitized on a scale of 0 to 255 using 8 binary digits. Two hundred such sectors were integrated and digitized along a given 2° azimuth region. A range delay of 29.6 km (16 nmi) was used. Digitizer calibration runs for the WSR-57 radar were normally made before as well as after each summer's experiment. Only one representative calibration was used for each entire season. Because this radar was operated continuously by the National Weather Service, its stability was rather high and only one calibration was needed to cover the period of each FACE experiment.

The first step in processing the data was to determine what was noise and what were valid data. True noise is expected to fluctuate randomly around a small value. A frequency distribution of digitized returned power values should show an approximately normal curve for the low values and scattered smaller frequency peaks for the much higher real returns. The data were processed to obtain a frequency distribution of the digitized values for each day. These distributions were carefully examined to determine the extent of noise. Normally, noise was defined to be all digitized values less than or equal to the mean plus three standard deviations of the approximately normal distributions of the small digitized values.

The proper calibration and the radar equation were used to assign a radar reflectivity value to every video data point whose digitized value was above the noise level. The resultant values were put into a data matrix, which constituted a low-level reflectivity map of the region.

The next step in processing the data was to correct for the range bias of the reflectivity due to detection failure and averaging restrictions. The first problem results from the fact that the intensity of the returned power from weak, distant targets falls either below the level of the minimum detectable signal or within the noise level of the system. As a result, only moderate and strong targets at large distances are detected, and a plot of dBz values versus range shows the average dBz increasing with range after 75 to 100 km. This detection bias occurs in addition to the averaging bias resulting from the spreading of the radar beam with range. Because of the widening beam, reflectivity cores are averaged out with weaker regions, resulting in lower apparent values with increasing range. This problem becomes worse when the echoes are small and do not fill the averaging unit (data bin) completely. No correction for the averaging bias was attempted. The correction procedure for the detection bias used the radar equation, calibration, and noise as input. The minimum reflectivity value at the most distant data bin that would have produced a return signal just above the noise level was calculated.

Any echo along the radial whose reflectivity fell below this value was neglected. Although some valid data were rejected in this procedure, the range bias was eliminated and the final data set was more statistically reliable and homogeneous.

Especially in the latter part of the afternoon, and on occasions when divergent downdrafts from large mature clouds were occurring, anomalous propagation (AP) of the radar waves could obliterate large regions of the echo field. Under these conditions, large ground return areas could be seen beyond the usual ground clutter region. The radar data were rejected if it was felt that the real echo returns were heavily contaminated by AP.

No attempt was made to correct for differences in radar beam elevation with range and the possible evaporation of the rain once it falls below cloud base.

The matrix of reflectivity values was transformed into one of rainfall rates using the FACE Z-R relationship (Woodley, 1970); i.e.,

$$R = (Z_e/300)^{1/1.4} \qquad (1)$$

where Z_e is the equivalent reflectivity in $mm^6\ m^{-3}$ and R the rainfall rate in $mm\ h^{-1}$. Woodley (1970) made use of the mesonetwork raingages (inner box in Fig. 1) to obtain a gage-to-radar ratio that was subsequently used to adjust the radar-derived rainfall. No adjustment was employed in this study, however. This matrix of rain rates constituted the primary data set for this study.

2.3. Radiosonde Data

Radiosonde data were obtained by the National Weather Service (NWS) at Miami (MIA) in 1975 and at West Palm Beach (PBI) in 1978. (The NWS moved the radiosonde site from MIA to PBI, a distance of about 100 km, in 1977.) A comparison made by the staff of the National Hurricane and Experimental Meteorology Laboratory (Cumulus

Group Staff, 1979) prior to the second phase of the FACE (1978-1980) revealed that the large-scale features of soundings taken simultaneously at MIA and PBI were very similar. Temperature differences below 300 mb were usually less than 1° C, and relative humidities were within 10% of each other. The basic synoptic features of soundings at both locations were similar. Most of the differences were observed in the boundary layer and responded to local phenomena. Therefore, since this study is concerned with the principal regional- and synoptic-scale meteorological factors associated with the convective activity over a large area, soundings from those two stations were considered together in deriving mean soundings for groups of days having similar convective activity. Data from both the standard mandatory levels (i.e., 1000 mb, 850 mb, 700 mb, 500 mb, 400 mb, 300 mb, 250 mb, 200 mb, 150 mb, and 100 mb) and significant levels were used. Additionally, radiosonde data from only mandatory levels were collected at weather stations located in the southeast United States, the Bahama Islands, Cuba, and the West Indies. The soundings used were all taken at 1200 UT (0800 EDT), because a later, afternoon sounding would probably reflect the changes in the atmospheric structure of the region produced by the convection itself, confusing the information about those environmental factors that are conducive to or attending the development of that convection.

2.4. Synoptic Weather Charts

Use was also made of standard surface and upper-air synoptic weather charts prepared and archived by the National Hurricane Center. These maps cover southeastern North America, the Gulf of Mexico, the Caribbean Sea, and most of the western Atlantic Ocean. Daily synoptic descriptions, published in the FACE data catalog series (Cumulus Group Staff 1976, 1979), were also used in this study.

3. ANALYSIS PROCEDURES

3.1. Radar Composite Maps

The radar rain-rate maps were used to determine the echo patterns on each of the days of the study. Computer programs were used to compute and sum up the rain rates at each of the 36,000 data points (180 two-degree sectors of 200 data bins each) for each scan (usually one every 5 minutes) for a period of 1 hour. A sum of the rain rate values, and the integer count of the number of zero and non-zero rain rate values was saved for each data bin. This process was repeated for all 12 hours of data for each day. Next, the summed rain rates and bin counters were used to compute both the average rain rate of the convection and the summed rain depth at each data bin. Henceforth, these two products will be referred to as option 1 and option 2, respectively. The 1-hour data matrices were combined to produce 3-hour (option 1) maps, and 12-hour (option 2) maps. The 3-hour maps covered four time periods: 0900-1200, 1200-1500, 1500-1800, and 1800-2100 EDT. These four time periods correspond roughly to the morning preconvection period; the early afternoon, developing convection period; the late afternoon, mature convection; and the early evening, dissipation stage.

Up until this point, all the data had been in polar coordinates. Conversion from polar to Cartesian coordinates was performed using the same transformation scheme that has been used in the FACE rainfall analysis. A detailed description of this process is found in Ostlund (1974) and Wiggert et al. (1976). This coordinate transformation results in a slight change in the radar-data domain. Initially, the data consist of 180 two-degree radials that contain 200 bins that are 930 m (0.5 nmi) in length. A range delay of 29.6 km (16 nmi) is employed. Thus, the data cover an annulus with an inner radius of 29.6 km

and an outer radius of 214.6 km (116 nmi). After the coordinate transformation, the domain consists of a 335.4 X 335.4 km (181 X 181 nmi) square, and each data bin measures 1.85 km (1 nmi) on a side. This results in a truncation of up to 48.2 km (26 nmi) of data along the 90°, 180°, 270°, and 360° radials, and lesser amounts along other radials. There will also be small regions of no data in the corners; the maximum data gap will be 23.5 km (12.6 nmi) along the 45°, 135°, 225°, and 315° radials. All subsequent computations were performed on this data grid. For presentation purposes, a strip measuring 111.2 km (60 nmi) along the eastern boundary and another measuring 83.4 km (45 nmi) along the southern boundary were omitted. Both of these strips lie over the ocean. The heavy line in Fig. 1 outlines the area for which radar data presentations are shown.

Next, 3-hour and 12-hour maps were generated, and an examination of the radar maps for each of the four time periods for each day followed, with the purpose of identifying recurrent convective pattern types.

3.2. Typing of Convective Patterns

In their study of Florida convection, Frank et al. (1967) stratified the study days by wind direction at the 1524 m (5000 ft) level using three radiosonde sites (Miami, Tampa, and Daytona Beach). The sector divisions of wind direction for the stratification were admittedly arbitrary and differed for each station. Because there is no physical basis for the divisions, and this author knows of no obvious scheme a priori for determining the sectors, it was decided to approach the problem from the other direction; that is, rather than stratifying the days by wind regime and determining echo patterns, the investigation becomes one of identifying echo patterns and determining the synoptic-flow regime. Thus, the decision was made to group the echo patterns into a set of types, and to study the wind and thermodynamic characteristics accompanying each echo type.

This decision having been made, the first step was to identify and determine the recurrent echo patterns and their development in time and space. Numerous varieties are present when small details are included but, in general, four basic types of convective patterns were found to be typically observed in south Florida.

Each day was then examined using the radar composite maps and was (subjectively) assigned to one of the four types. This process resulted in assignment of 37 days to Type 1, 24 days to Type 2, 23 days to Type 3, and 30 days to Type 4, for a total of 114 days. A composite was prepared for all days within one type and checked to see if the distinctive patterns that initially determined the grouping of each day were maintained. There was some "spreading out" of the patterns in the composites, which is to be expected, since there will be small temporal and spatial variations between individual days even within each type. In general, however, the patterns held up well in the compositing scheme.

Examination of the different patterns also revealed certain areas consistently exhibiting either higher or lower radar reflectivity values than the surrounding areas, regardless of the pattern. It is believed that the circulations developed by the interaction of the different scales (regional, synoptic, peninsular) are locally modified by inhomogeneities in the underlying terrain to produce these geographical variations in intensity.

3.3. Mean Soundings

A mean sounding was constructed for each of the four types by averaging together all the 1200 UT (0800 EDT) PBI and MIA soundings for the days determined from the radar data to belong in each group. The data were interpolated to 50-mb intervals before averaging. Next, all the days used in the study were averaged together to get the mean atmospheric sounding for the two summers. The mean for each group, and the difference between the mean of each group and the overall mean, were computed. Parameters calculated included the u- and v-components of the vector wind, the wind direction and

wind speed, temperature, equivalent potential temperature, and mixing ratio for each level. These parameters were plotted in two ways: (1) as the mean of each parameter for each of the four types to determine the basic relationships between them, and (2) as the difference between the mean of each group and the mean of all days taken together for each parameter. This method of presentation is similar to that used by Lopez et al. (1983b) in their study of Florida convection.

Next, utilizing only the mandatory levels from all the regional stations, mean vector winds and u- and v-components of the wind were computed for each type. These winds were used in a modified Cressman (1958) analysis scheme to produce a streamline analysis in order to determine the typical regional- and synoptic-scale circulation features present for each of the four convective pattern types.

Once the individual days were stratified into four distinct types, and mean soundings and streamline analyses were computed for each of these, it remained to be shown that there was, in fact, a distinct synoptic pattern that could be associated with each type. Not only should it be a distinct pattern, but it should be one that can be easily and quickly recognized by visual observation of the standard synoptic charts.

4. RESULTS

4.1. Total Season Rainfall

One of the first results obtained was the total season rainfall for the period 0900-2100 EDT. This product is the sum of the 12-hour, option-2 (rain depth) data matrices for all the days. The result of this summation (Fig. 2) is a map depicting the mean of the 1975 and 1978 total season (1 July - 31 August) rainfall and contoured for rain depths of 175 mm, 250 mm, and 350 mm. From this map, it is clear that the land mass plays an important role in the generation of convection. There is a strong and well-defined gradient of rainfall along the west coast. Although not as sharp, there is also a strong rainfall gradient along the east coast. This is not surprising, nor is it a new finding, having been noted first by Byers and Rodebush (1948) and by numerous investigators since then. What is interesting, though, is the non-uniformity of the rainfall distribution. A number of areas exhibit well-defined maxima or minima. Some of these maxima/minima are easily related to features such as the sea breezes, but others are not so readily apparent. A combination of large-scale flow, peninsular-scale circulation, and local surface features must play some role in producing the observed variations in the rainfall amounts.

Figures 3, 4, and 5 are simplified representations of the principal landforms, soils, and vegetation of south Florida; Fig. 6 shows the locations of the major water conservation areas in south Florida. These conservation areas are large bodies of relatively shallow water fed and drained by canals. The locations of the three water conservation areas in southeast Florida and the locations of rainfall minima suggest that the local minima along the southeast coast may be partly due to these water bodies.

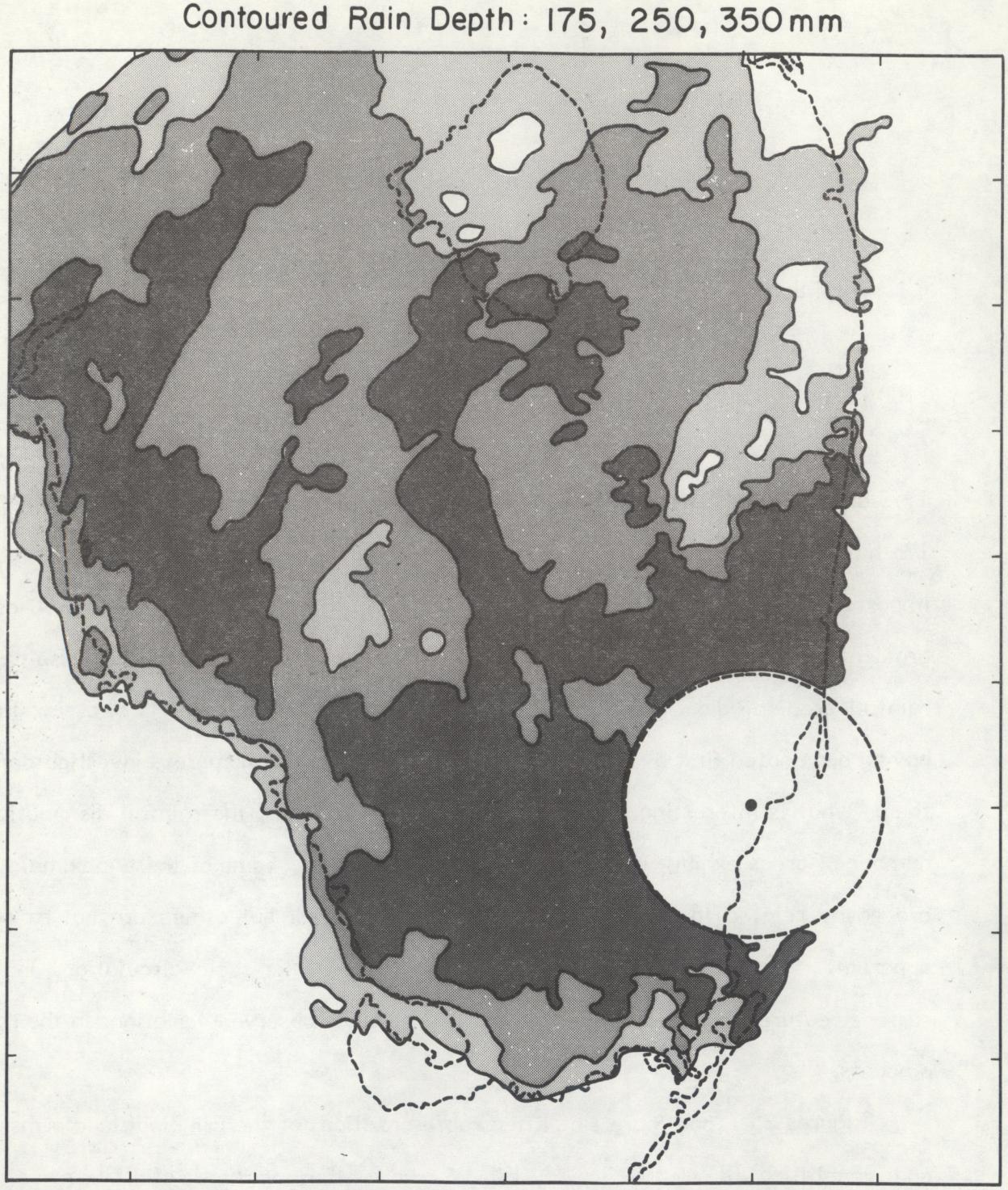

Figure 2. Total season (July-August) rainfall map of south Florida. Light shading represents depths greater than 175 mm, medium shading greater than 250 mm, and heavy shading greater than 350 mm. In this and all subsequent radar depictions, the circle in the lower right corner is the region of the 16 nmi radar range delay.

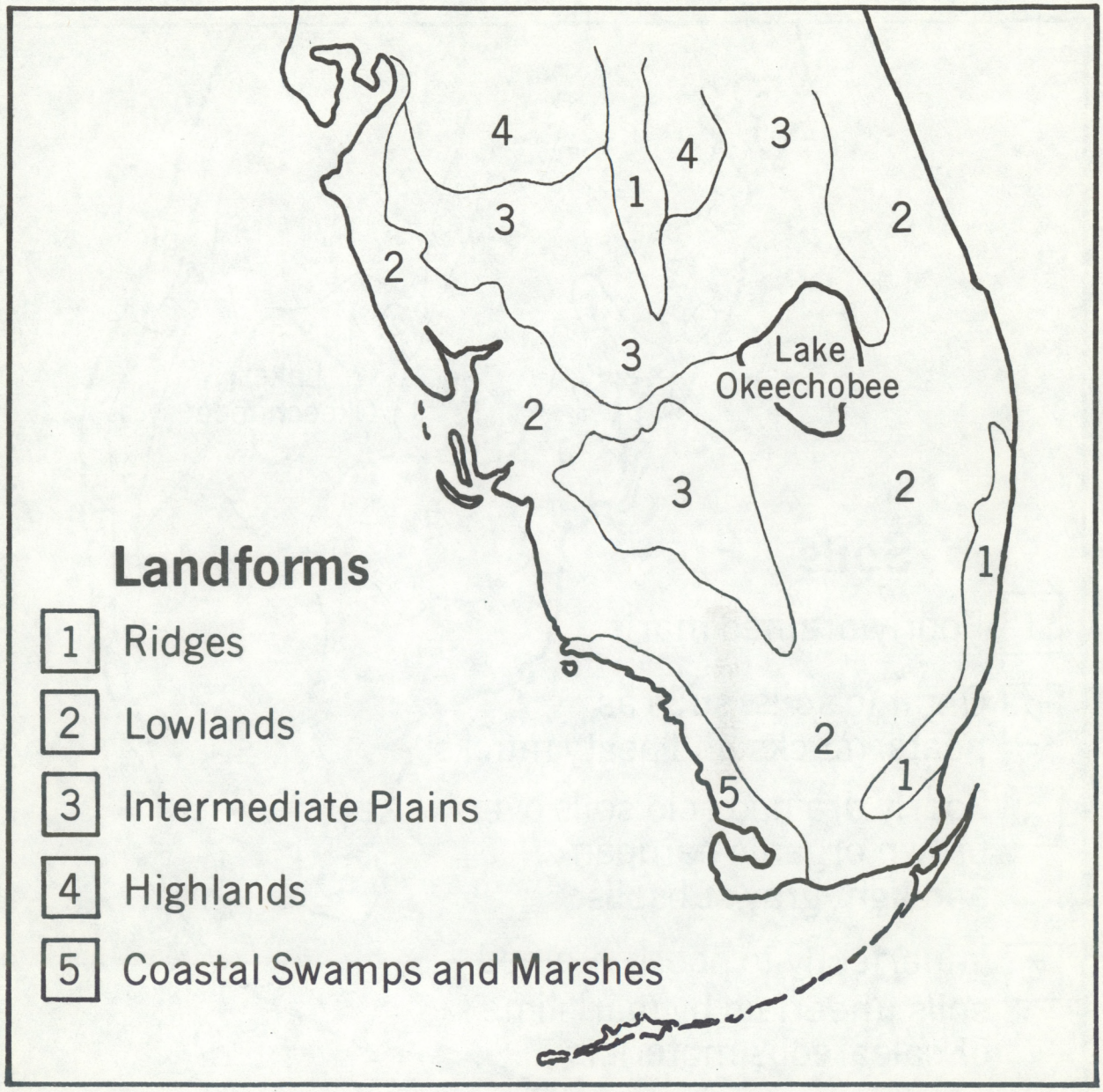

Figure 3. Principal landforms of south Florida (adapted from Wood and Fernald, 1974).

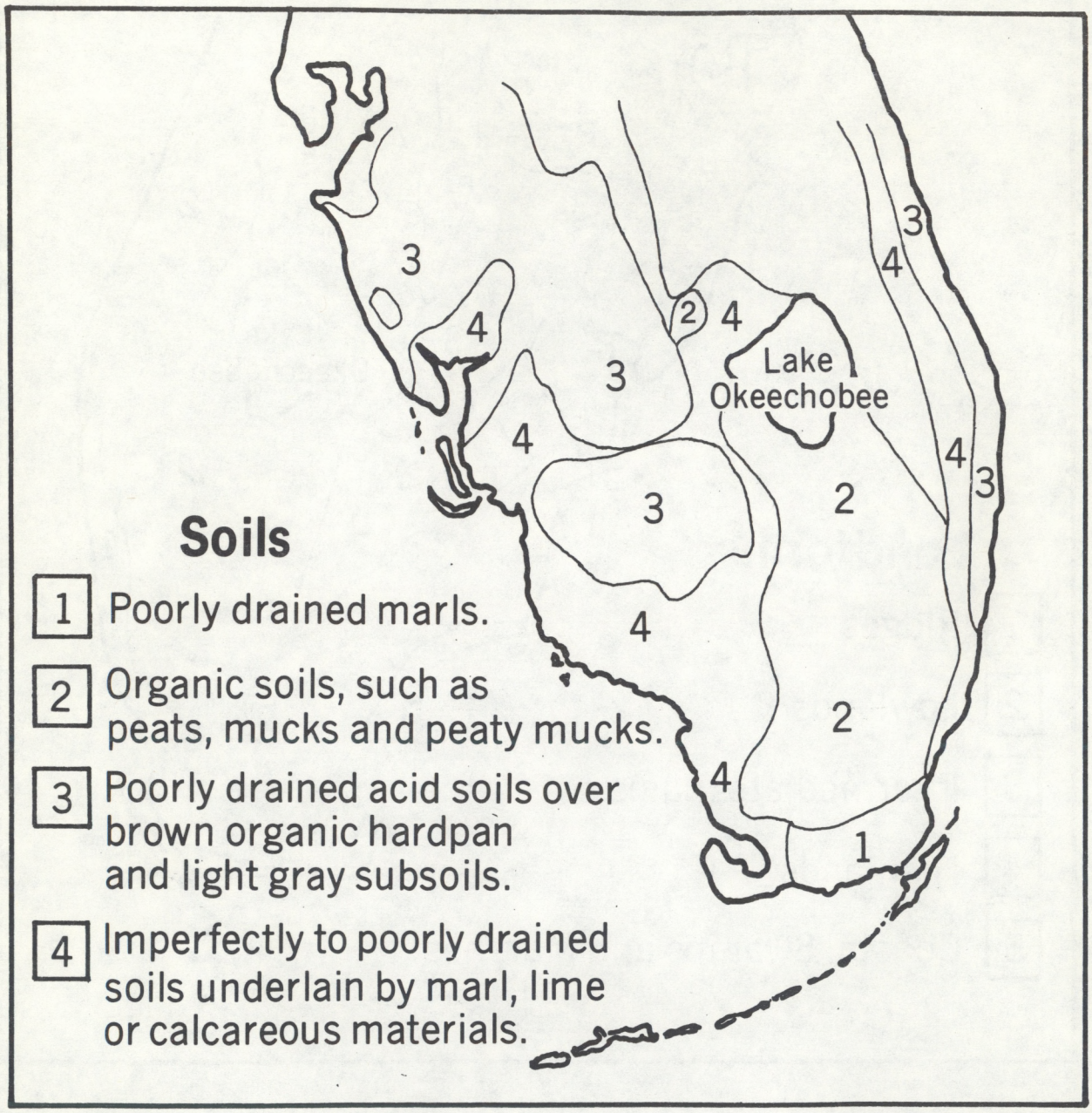

Figure 4. Principal soils of south Florida (adapted from Wood and Fernald, 1974).

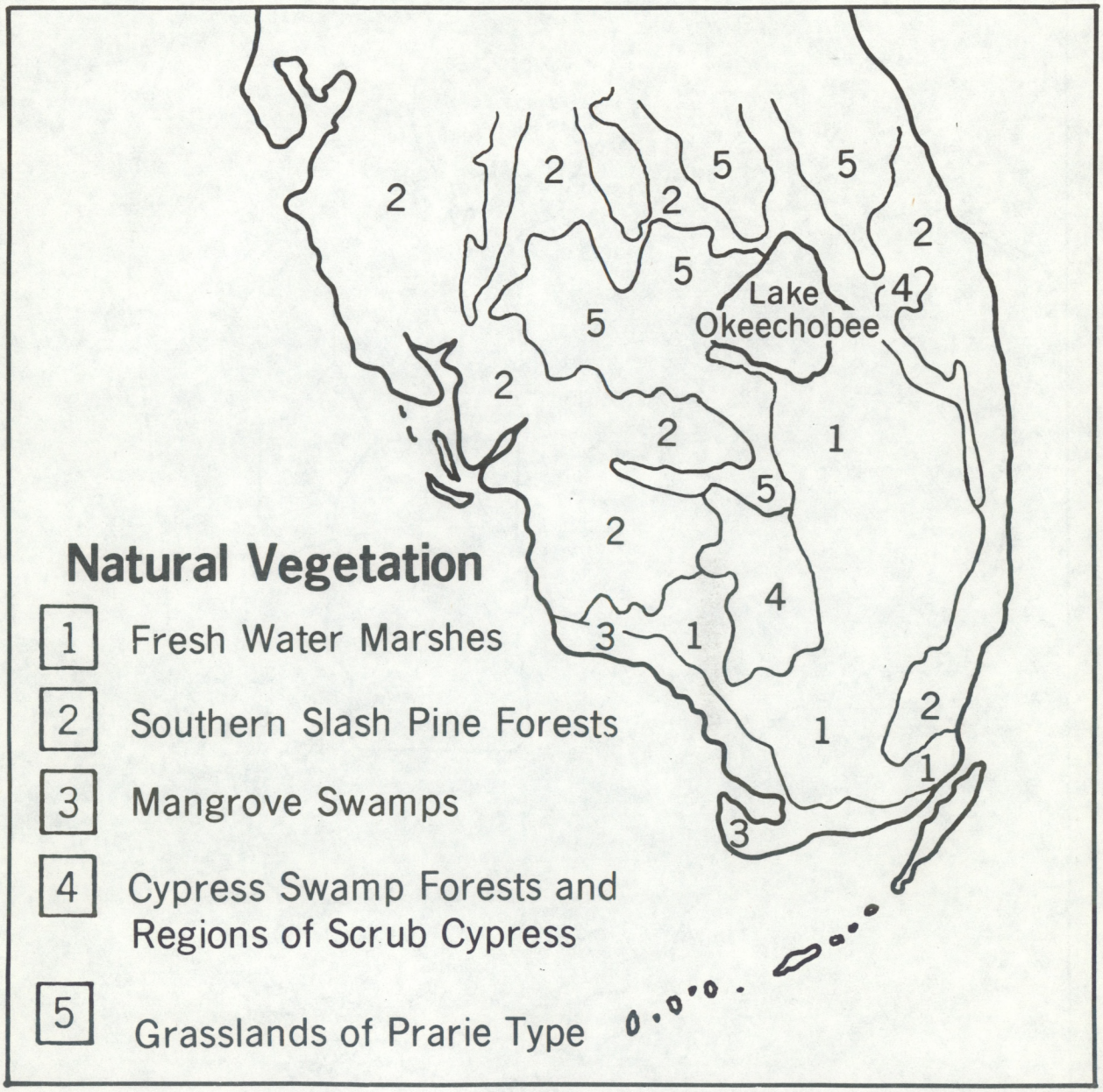

Figure 5. Principal vegetation types of south Florida (adapted from Wood and Fernald, 1974).

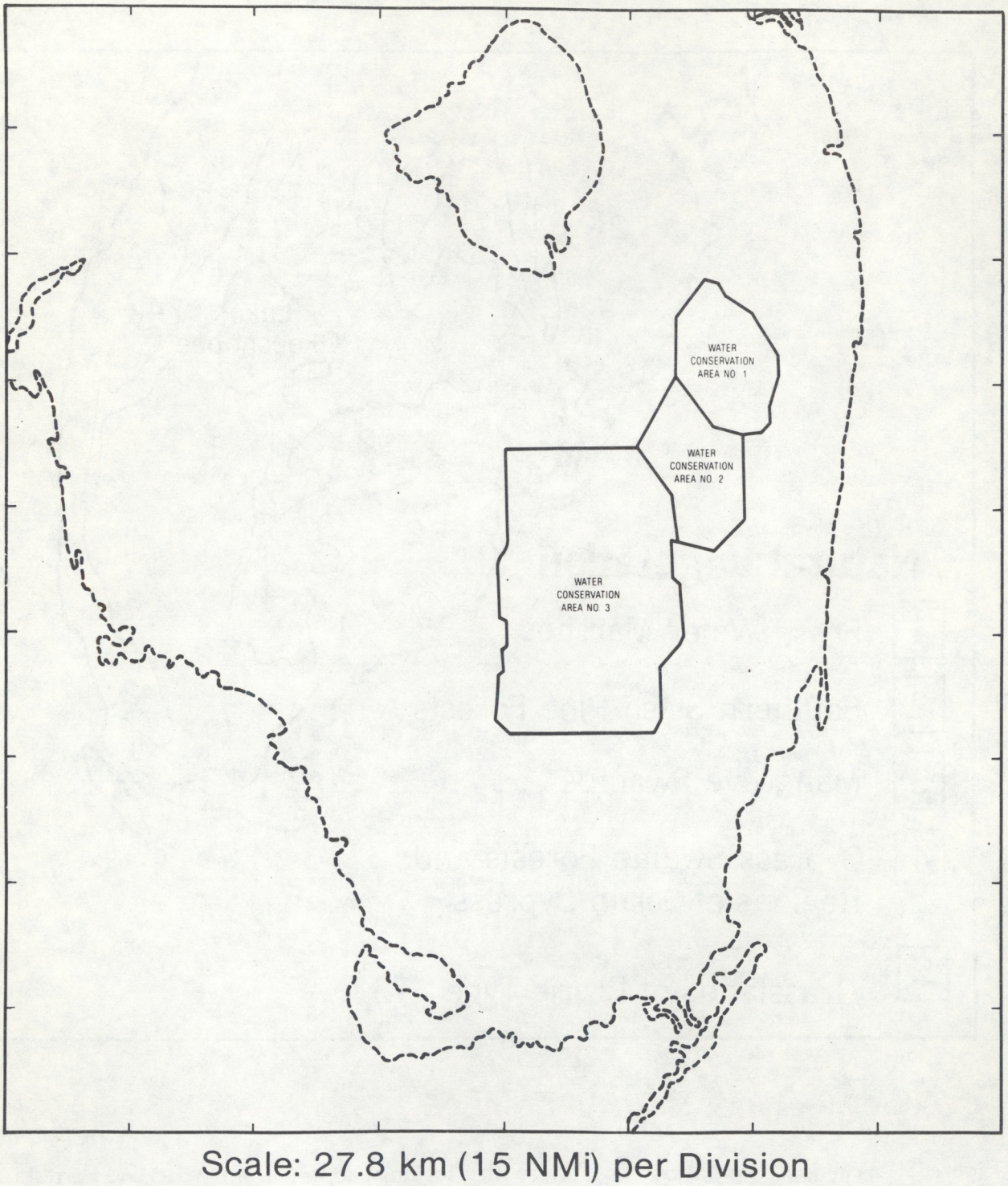

Figure 6. Water conservation areas of south Florida.

Since the thermal capacity of water is much greater than that of the surrounding land, the water warms at a slower rate than the neighboring ground. There is a decreased likelihood for thermal updrafts to form in this region. Also, as an already existing convective element passes over these water bodies, there is a tendency for the cloud to collapse temporarily as the warm updraft is extinguished.

Along and inland of the southwest coast of south Florida is the Big Cypress Swamp, another large body of water similar to the water conservation areas with one exception: there is considerable vegetation including many cypress trees, as opposed to the water conservation areas which are primarily areas of partially submerged grasses (see Fig. 5). The rainfall distribution map shows a rainfall minimum inland of the southwest coast, suggesting that it may be related to the large expanse of water within the swamp.

The largest water body in south Florida (and the second largest freshwater lake entirely within the United States) is Lake Okeechobee, located in the northern portion of the study area. The minimum in rainfall is very obvious from Fig. 2. Equally important is the extension of the minimum to the northwest, north, and northeast of the lake. This is the so-called "rain shadow". Pielke (1974) has shown that there is a subsidence region both over and downwind of the lake for a considerable distance. Additionally, the cooling effect of the lake probably plays some role in producing the observed "rain shadow". During the summer months, most days have a southerly component to the wind; hence the downstream side of the lake is to the north. (See Section 4.5.2 for a complete discussion of the prevailing winds.)

It is not immediately obvious from the observed rainfall what role the other variations of soil and vegetation play. Gannon (1978) and McCumber (1980) have shown with their sea-breeze models that the location, timing, and intensity of the sea-breeze convergence zones are related not only to the different soils and vegetation types but also, just as importantly, to the transition zone between neighboring regions. It is in these regions that there is a tendency to produce surface moisture gradients, causing

differential heating to take place. This differential heating, in time, may set up a secondary circulation not unlike that of the sea breezes. After the convection has been initiated, it may remain anchored to its region of origin or move with the prevailing winds. This motion will spread the rainfall over an area downwind of the generation zone. It is partly for this reason that the patterns of total season rainfall seem to be only slightly related to the underlying vegetation and soil, whereas a map depicting the convective generation zones would probably show a better correlation .

4.2. Description of the Four Convective Pattern Types

It has been shown by investigators that the Florida sea breeze is usually accompanied by a narrow band of convergence and upward vertical motion resulting in the development of convective elements embedded within the sea breeze (Pielke, 1973, 1974; Pielke and Mahrer, 1978; Gannon, 1978; Burpee, 1979; McCumber, 1980; Burpee and Lahiff, 1983). On the basis on these observational and numerical studies, convective lines that form parallel to the east or west coast of Florida in the accompanying radar composite maps are determined to be sea-breeze related and are designated the east or west coast sea-breeze convergence zones.

The radar presentations (Figs. 7-10) shown in the following sections are all option-1 (mean rain rate) composites.

4.2.1. Type I

Type I days (Fig. 7) are the most convectively organized. Early in the day (0900-1200 EDT), the east coast sea breeze develops as indicated by scattered convection near the east coast. During the second time period (1200-1500 EDT), major development of convection takes place along both coasts. The east coast sea breeze (ECSB) becomes more convectively active and begins to move inland. During this same period, the west coast sea breeze (WCSB) develops. Note that in the composite, the ECSB convection,

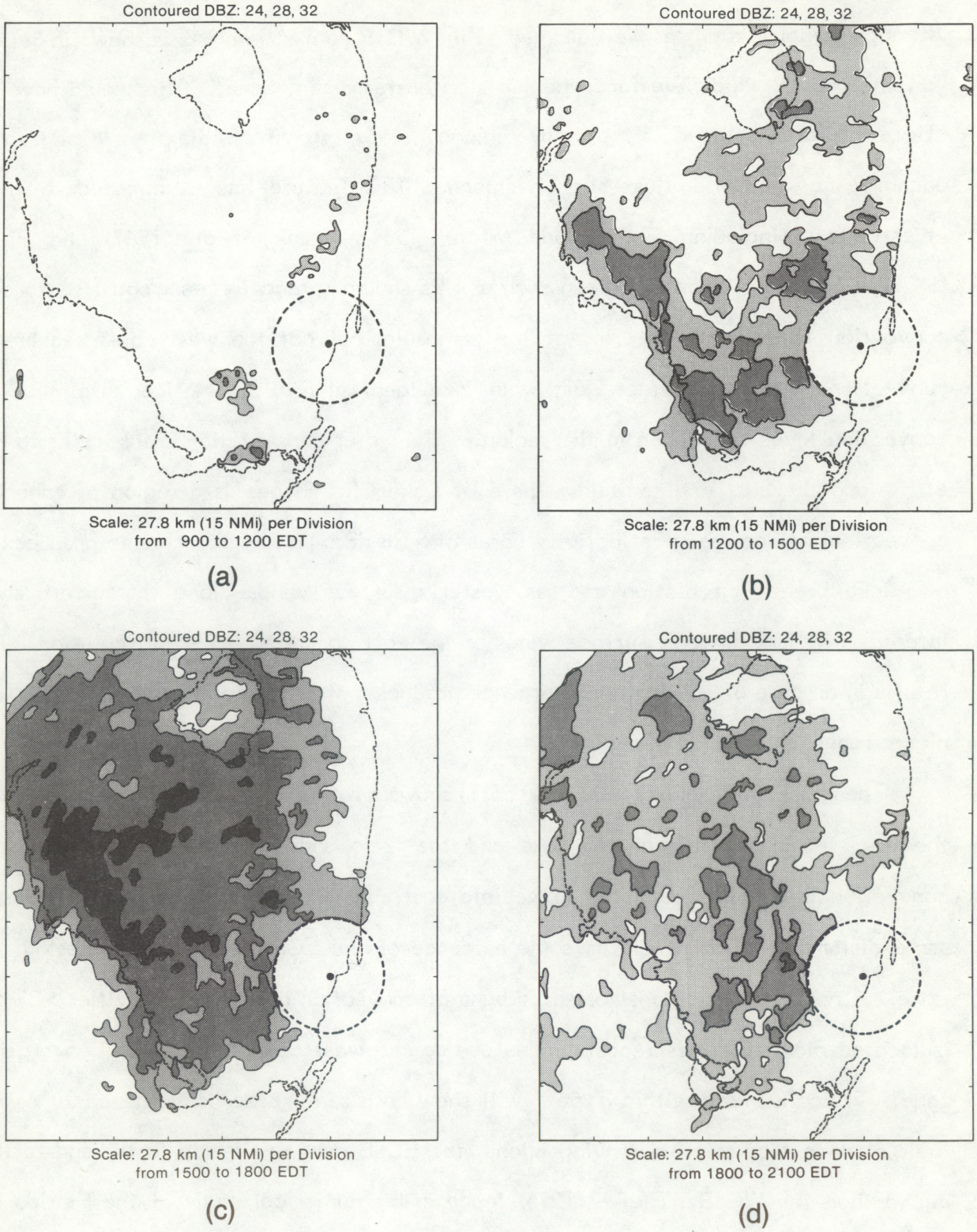

Figure 7. Convective patterns over south Florida for Type I days for (a) 0900-1200, (b) 1200-1500, (c) 1500-1800, and (d) 1800-2100 EDT. Light shading is for radar reflectivities of 24 dBz, medium shading is for 28 dBz, and heavy shading is for 32 dBz.

although obvious, is not as well defined as the WCSB convection. As is shown in Section 4.6, the typical wind field for Type I has an easterly component. This would have the effect of forcing the ECSB to move inland during the day, while the WCSB remain anchored to a position just slightly inland. This feature has been noted by many investigators, including Gentry and Moore (1954), Frank et al. (1967) and Pielke (1973,1974). Thus, a 3-hour mean such as this should spread the east coast sea-breeze convection towards the interior of the peninsula, but not the west coast sea breeze convection. This is, in fact, just what is evident in Fig. 7. Notice, also, that the convection tends to weaken in the region of the water conservation areas (refer to Fig. 6). Along the east and southeast shore of Lake Okeechobee is a region of enhanced convection, having mean reflectivity cores of $\geq$ 28 dBz. Lake Okeechobee produces its own lake breeze circulation and its westerly surface winds along its eastern shore interact with the easterly surface winds of the east coast sea-breeze circulation. This results in an area of enhanced convergence producing stronger convective elements with higher radar reflectivities.

The third time period (1500-1800 EDT) shows a rather large spread of echoes. Note the weak echo region over the lake and the "rain shadow" to the northwest. No convection is evident along the immediate east coast; however, convection is present some distance inland. There is some evidence of the ECSB located southwest of the Lake. A northwest-southeast oriented band of convection having reflectivities $\geq$ 32 dBz is located along the west coast and is due to the west coast sea-breeze convergence zone. Typically, days within Type I will show both sea-breeze convergence zones and their attendant convection moving inland, the ECSB moving slightly faster and farther inland than the WCSB. Pielke (1974) found in his numerical study of the Florida sea breezes that under a southeasterly flow the ECSB convergence zone moves inland slowly at first, but accelerates later. At some point during the afternoon, these two convergence zones usually merge and convection aligns in a general north-south

orientation along the line of the merger. This merger, more often than not, takes place to the west of the center of the peninsula as a result of the synoptic-scale flow from the southeast.

The last time period (1800-2100 EDT) is primarily the dissipation period for the convection and the sea-breeze convergence zones. Most convection at this time is well away from the east coast and extends from the interior all the way to the west coast. The strongest reflectivity cores ($\geq$ 32 dBz) are located in the center and to the west of the center of the peninsula and are the remnants of the merged sea-breeze lines.

Type I convection is characterized by early development of convection within the east coast sea-breeze convergence zone, followed some time later by convection within the west coast sea-breeze convergence zone. Both sea breezes advance inland; however, the ECSB moves faster and farther than the WCSB. Merger of these two sea breezes usually takes place inland in the center or to the west of the center of the peninsula. The strongest convection, in the interior of the peninsula, finally begins to diminish during the early evening.

4.2.2. Type 2

Type 2 days (Fig. 8) start out in a fashion similar to the Type I days, but many differences develop. During the period from 0900-1200 EDT, the ECSB convergence zone has convection in progress, but the amount of radar echo is considerably less than that of Type I during the same time period. Even by the second period (1200-1500 EDT) convection is sparse. The ECSB has moved inland a considerable distance so that the northern portion is along the east shore of Lake Okeechobee and the southern portion is oriented slightly west of due south (i.e., it is parallel to the curved east coast). Some very isolated convection is taking place along the west coast, but there is no organized WCSB convection.

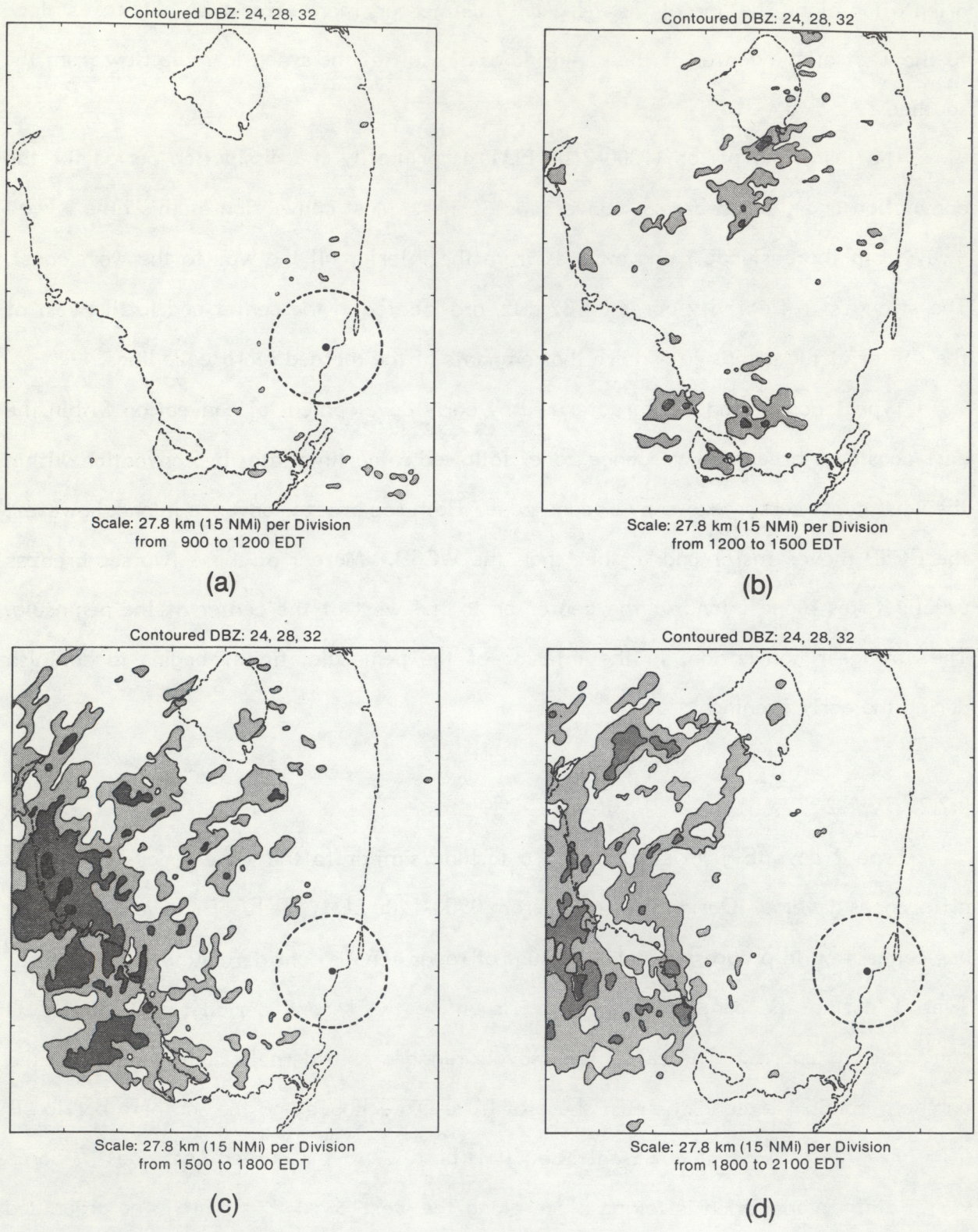

Figure 8. Convective patterns over south Florida for Type 2 days for (a) 0900-1200, (b) 1200-1500, (c) 1500-1800, and (d) 1800-2100 EDT. Shading same as in Fig. 7.

In the period from 1500-1800 EDT, convection becomes more widespread, but is concentrated in the western half of the peninsula. A few showers linger along the east shore of the lake and are probably related to the lake breeze. Along the west coast a merger of the ECSB and WCSB has taken place with strong convection finally developing. Highest reflectivities are located in the strongly curved portion of the southwest coast. This convex curvature of the coastline tends to concentrate and enhance the sea breeze (Neumann, 1951; McPherson, 1970; Smith, 1970; Pielke, 1974), and it is not surprising that this region experiences stronger convection. Additionally, the concave coastline just to the south tends to have the opposite effect, resulting in weaker convection. By the last time period, the synoptic-scale easterly winds (described in detail in Section 4.6) have advected the convection off the west coast and into the Gulf of Mexico. These results agree quite well with the results of Pielke's (personal communication, 1983) model runs for easterly winds.

In summary, Type 2 convection starts along the east coast, is quickly advected to the west coast where the two sea-breeze convergence zones merge, producing strong convection which is locally modified by the curvature of the coastline, and finally, is advected out to sea.

4.2.3. Type 3

On Type 3 days (Fig. 9) convection starts earlier than on Type 1 or Type 2 days. In the morning (0900-1200 EDT), both the ECSB and WCSB convergence zones generate convection, and a third area of convection is present to the west of the lake. Convection spreads quickly, and by the second period (1200-1500 EDT) a major portion of the peninsula is convectively active. There is a region of higher reflectivity oriented northwest-southeast along the west coast that is associated with the WCSB, and another one oriented north-south along the east coast that is related to the ECSB. There is a distinct "rain shadow" to the northeast of Lake Okeechobee. Note that the WCSB has

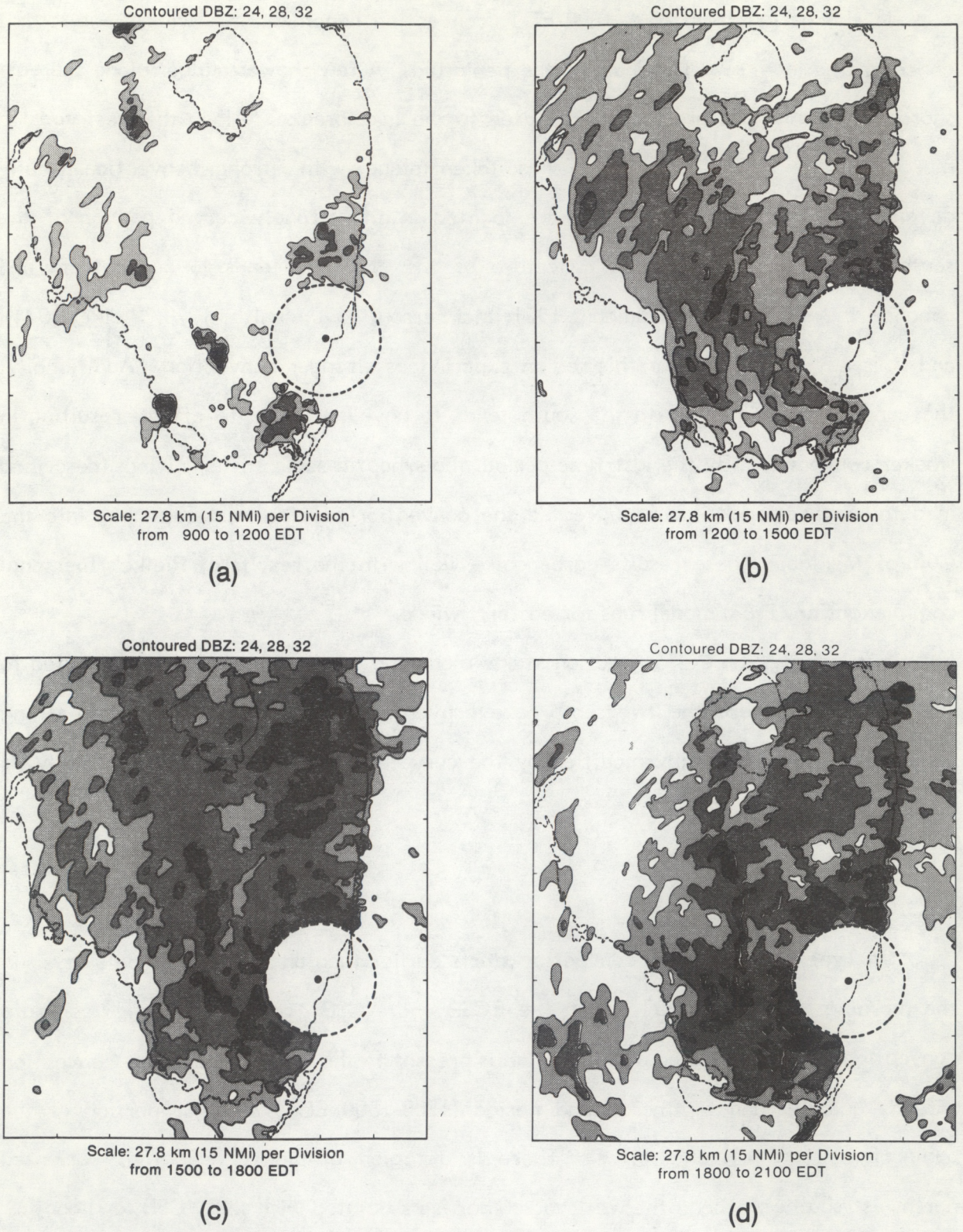

Figure 9. Convective patterns over south Florida for Type 3 days for (a) 0900-1200, (b) 1200-1500, (c) 1500-1800, and (d) 1800-2100 EDT. Shading same as in Fig. 7.

moved inland while the ECSB has remained essentially stationary. As is shown in Section 4.6 in more detail, the mean wind for Type 3 is from the southwest, so it should be expected that the WCSB would move inland with the mean synoptic flow, while the ECSB remains close to the coast.

By the next period (1500-1800 EDT), convection has weakened along the west coast as the convergence zone moves farther inland. The WCSB convergence zone is located in the central portion of the peninsula, while the ECSB still remains anchored along the east coast. This pattern is not unlike a mirror image of Type 1. A difference here is that the ECSB does not propagate inland to meet the WCSB in the interior. A possible explanation for this phenomenon is that the mean wind speed for Type 3 days is higher than that of Type 1. This would tend to hold the sea breeze along the coast because the forcing from the sea breeze is not sufficient to overcome the synoptic-scale flow. Finally, during the evening (1800-2100 EDT), convection has all but ended along the west coast, but continues quite vigorously in the interior, and especially along the east coast. There is a relatively narrow but strong band of radar echoes located directly on the coastline, and a secondary maximum to the west. Some convection is evident offshore of the east coast. Again, this pattern agrees quite well with the results of Pielke (1974).

Type 3 days are typified by an early onset of convection along both coasts. The west coast sea breeze moves inland during the day, while the ECSB remains anchored to the coast. Later in the day, the WCSB merges with the ECSB producing a strong north-south line of echoes along the east coast. Dissipation usually takes place late in the evening. In contrast with Type 1 and Type 2 days, the Type 3 days exhibit a higher echo area coverage and dissipation takes place much later in the day. This result can be explained in terms of the synoptic setting in which Type 3 days occur. This setting is described in detail in Section 4.6.

4.2.4. Type 4

The days that constitute Type 4 are actually a mixed group subject to many types of disturbances, including tropical disturbances (easterly waves, tropical depressions, etc.), westerly disturbances (middle-latitude short waves, dissipating cold fronts, etc.), and upper tropospheric cold lows. Type 4 also includes those days that can be characterized as being very tropical in their thermodynamic structure (i.e., having a deep layer of moisture, very high and cold tropopause, etc. (Jordan, 1958)). Each of these synoptic subdivisions affects the convective patterns in different ways. Looking at Fig. 10, we see that during the first time period the bulk of the convection is in the eastern half of the peninsula and over the Atlantic Ocean. The areal coverage of echoes is quite large for this time of day. Note especially the northwest-southeast banding that is present during the morning hours of days with easterly waves. Typically, convection is most active during the early hours of these disturbed days. During the next time period (1200-1500 EDT), there is a marked change in the convective pattern. The entire southern peninsula has echoes over it The stronger echoes ($\geq$ 28 dBz) are in bands oriented northeast-southwest; this is a 90^{o} departure from the orientation of the bands in the morning. Westerly type disturbances, most notably low-level convergence zones that are the remnants of cold fronts, push southward into the area and the zones of convergence associated with them are typically oriented northeast-southwest, relating well to the convective patterns. Note that the regions of lower reflectivity again seem to correspond quite favorably with the larger water bodies in south Florida. By late afternoon, the overall intensity of the convection has increased; we now see a larger area of reflectivity $\geq$ 28 dBz. Interestingly enough, there appears to be a fairly well defined east coast sea breeze located just east of Lake Okeechobee and extending south and then southwest to the lower southwest coast of Florida. Additionally, there is some indication of a west coast sea breeze as evidenced by the northwest-southeast region of higher reflectivities. Apparently, despite the disturbed nature of the day, there is sufficient

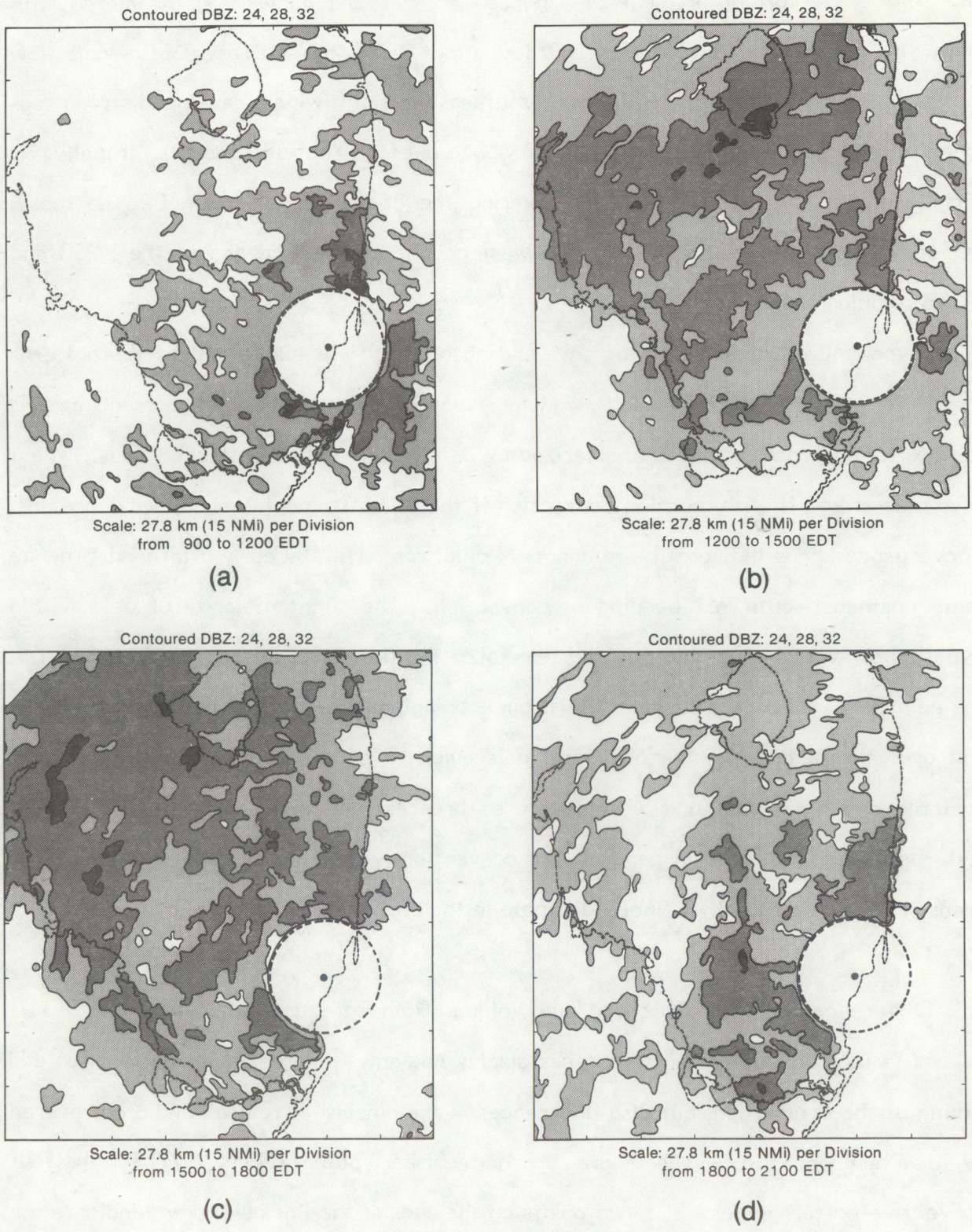

Figure 10. Convective patterns over south Florida for Type 4 days for (a) 0900-1200, (b) 1200-1500, (c) 1500-1800, and (d) 1800-2100 EDT. Shading same as in Fig. 7.

peninsular-scale forcing to generate the sea breezes and convection associated with them. In fact, Burpee and Lahiff (1983) found that those days with a synoptic-scale flow that paralleled the peninsula (i.e., south-southeast to south winds) developed strong sea-breeze convergence zones that produced above-average rainfall amounts. Finally, by early evening, the amount of echo covering the peninsula has started to decrease, especially along and just inland of the west coast. Little evidence of the ECSB and WCSB remains at this time.

Type 4 is a mixed group of days and no one day will exhibit all of the patterns shown for the four time periods. Many types of disturbances are present in this composite, and each type is characterized by its own convective patterns. Thus, Type 4 days may start off with morning convection if there is a tropical easterly wave present. Convergence zones that are the remnants of cold fronts will, by early afternoon, produce some northeast-southwest banding of convection. The slight majority of days within Type 4, however, are disturbed in the sense that the flow is southeasterly and parallel to the peninsula, and a deep layer of moist air is being advected straight out of the tropics and over the peninsula. Surface heating is quick to trigger convection in this moist, unstable air. The east and west coast sea breezes may often develop within these disturbed situations, but, in general, the convection will be widespread and have large areas of echo coverage that finally dissipate in the late evening.

4.3. Differences in Radar-Observed Rain Volume, Rain Rate, and Echo Area

The four convective pattern types display not only differences in the location and timing of the convection, but also differences in the amount of rainfall and area covered by radar echoes. Figures 11-18 are "box-and-whisker" plots (Tukey, 1977) for the four convective pattern types. The two points on the ends of the lines (whiskers) indicate the extreme values, while the bars correspond to the 25^{th}, 50^{th}, and 75^{th} percentiles. Thus, the boxed-in area shows where the central 50% of the values occur. Figure 11 shows the

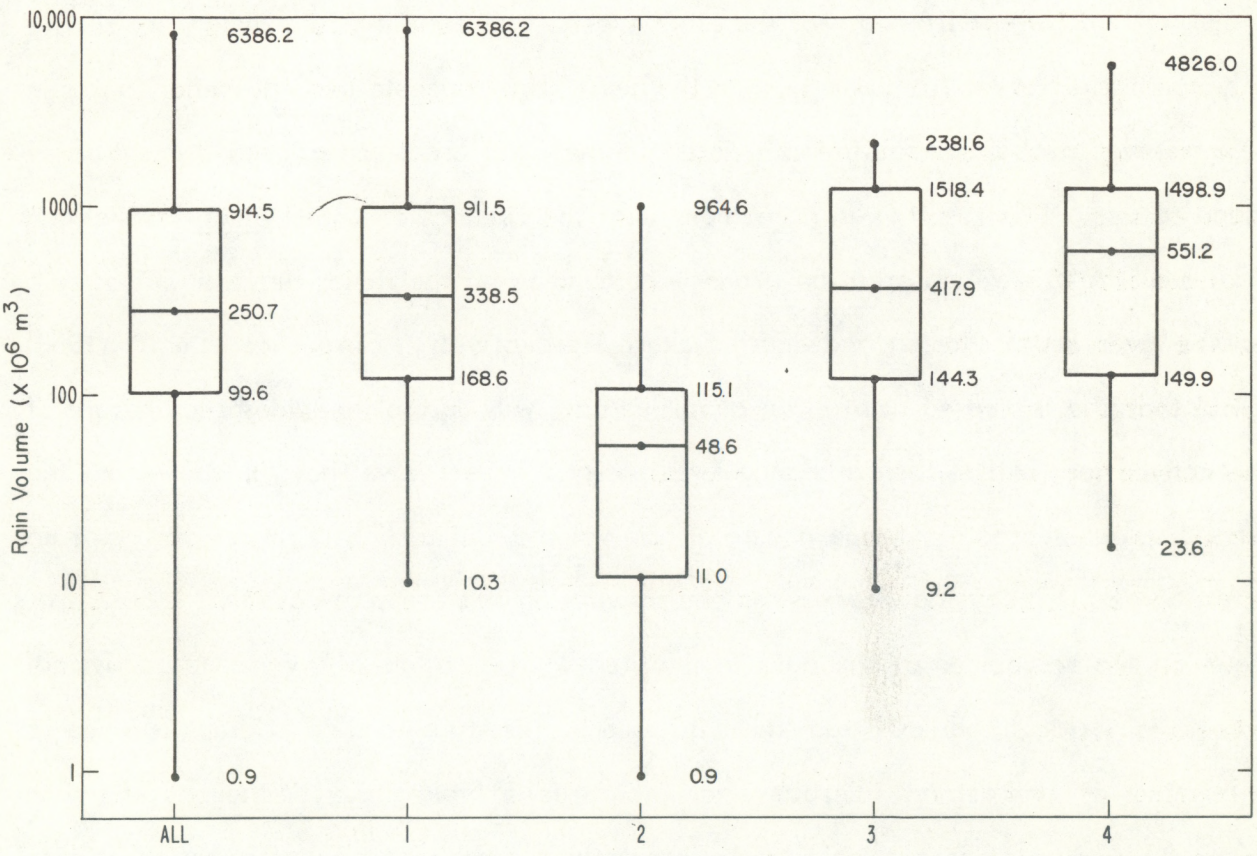

Figure 11. "Box-and-Whisker" plot of radar rain volumes. The points at the ends of the lines (whiskers) represent the extreme values; the three bars correspond to the 25th, 50th, and 75th percentiles. Thus, the boxed-in area shows where the central 50% of the values occur.

relationship of rain volume as measured by radar between the different types. It is immediately clear that Type 2 days experience considerably less rainfall than do any of the other types. There are differences between the other types also, but they cannot be considered very important. Figure 12 represents average echo areas. Here, again Type 2 is distinctly different from any of the other types. Interestingly, rain rates (Fig. 13) are only slightly different from one type to the next. This suggests that the major factor in determining total areal rainfall is related to the total areal coverage and duration of radar echoes. This result is in agreement with the findings of López et al. (1983c) and Doneaud (1981) in which areal coverage was found to be the major determinant of rain volume over south Florida and South Dakota, respectively. Burpee and Lahiff (1983) found that the increased rainfall on disturbed days was due to the widespread nature of the convection, rather than a change in intensity. Type 1 days show, in the mean, the second smallest areal coverage and total rain volume, but a slightly higher average rain rate. Some microphysical process may be at work on this group of days that is absent or weak on the remainder of the days in the study. The nature of such a microphysical process is not at all obvious from the data used in this study, and no attempt is made to determine or understand microphysical processes in this study, although numerous (aircraft) data sets are available to the interested researcher who desires to investigate these processes.

4.4. Wind Direction and Speed

Figures 14 and 15 are "box-and-whisker" plots of the mean layer vector wind (MLVW) direction and speed for each of the four types and for all types together. The MLVW is defined as the vector mean of the wind in the layer from 305 m (1000 ft) to 700 mb in 305-m intervals. The wind direction is computed from the u- and v-components, as is the wind speed. This layer was chosen because Woodley et al. (1982) have shown that echo motion in south Florida is related quite well to this mean wind and additionally (as

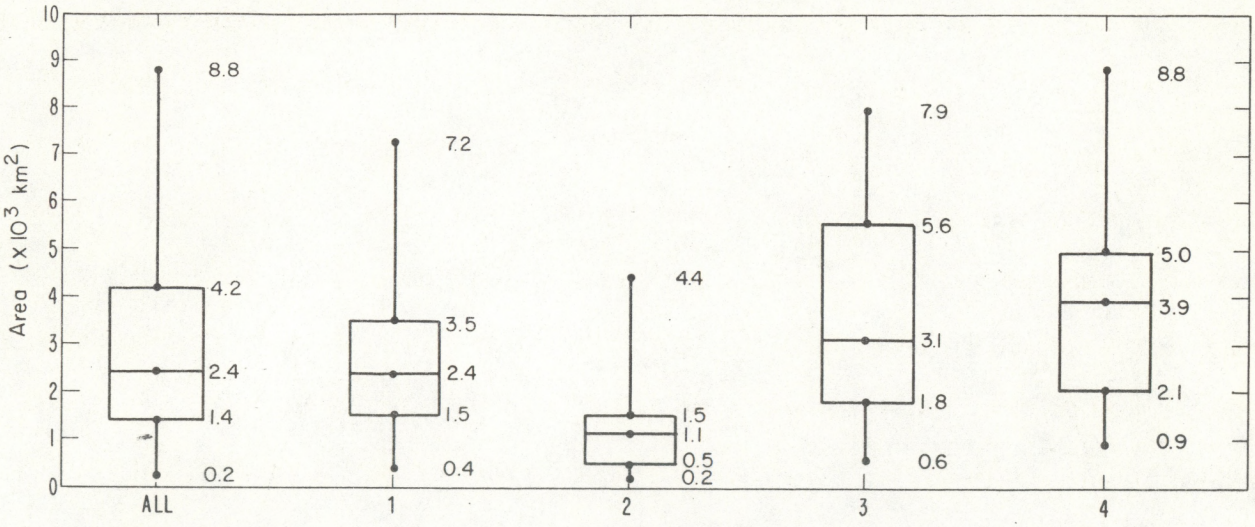

Figure 12. "Box-and-Whisker" plot of radar echo areas (see legend of Fig. 11).

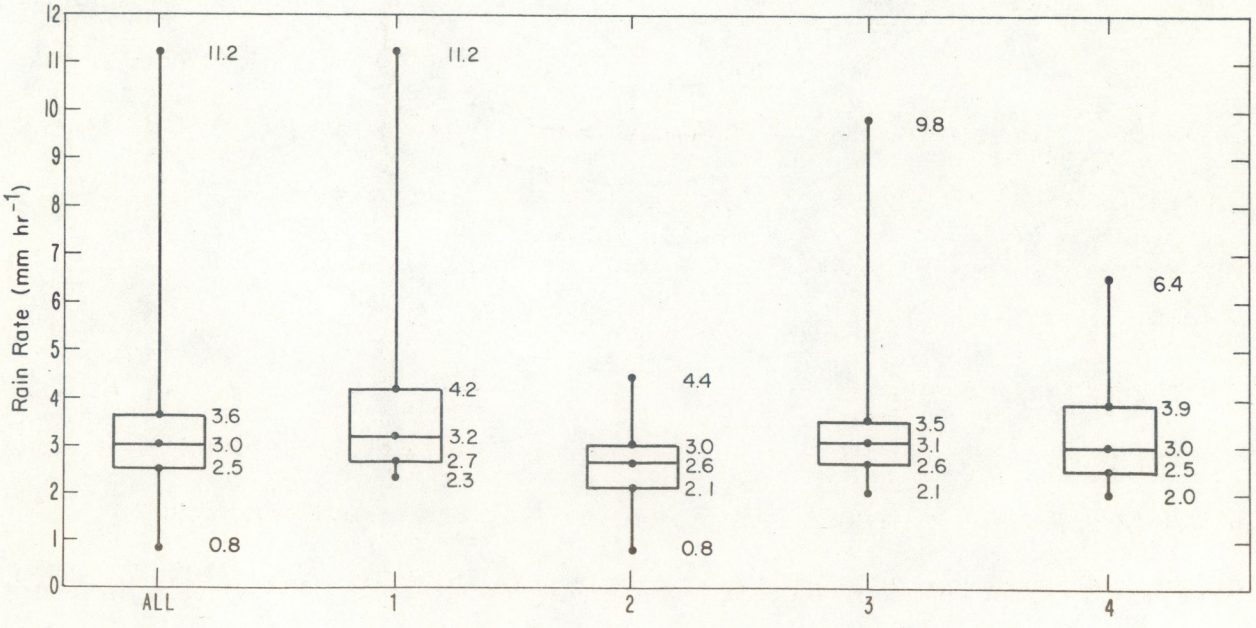

Figure 13. "Box-and-Whisker" plot of radar rain rates (see legend of Fig. 11).

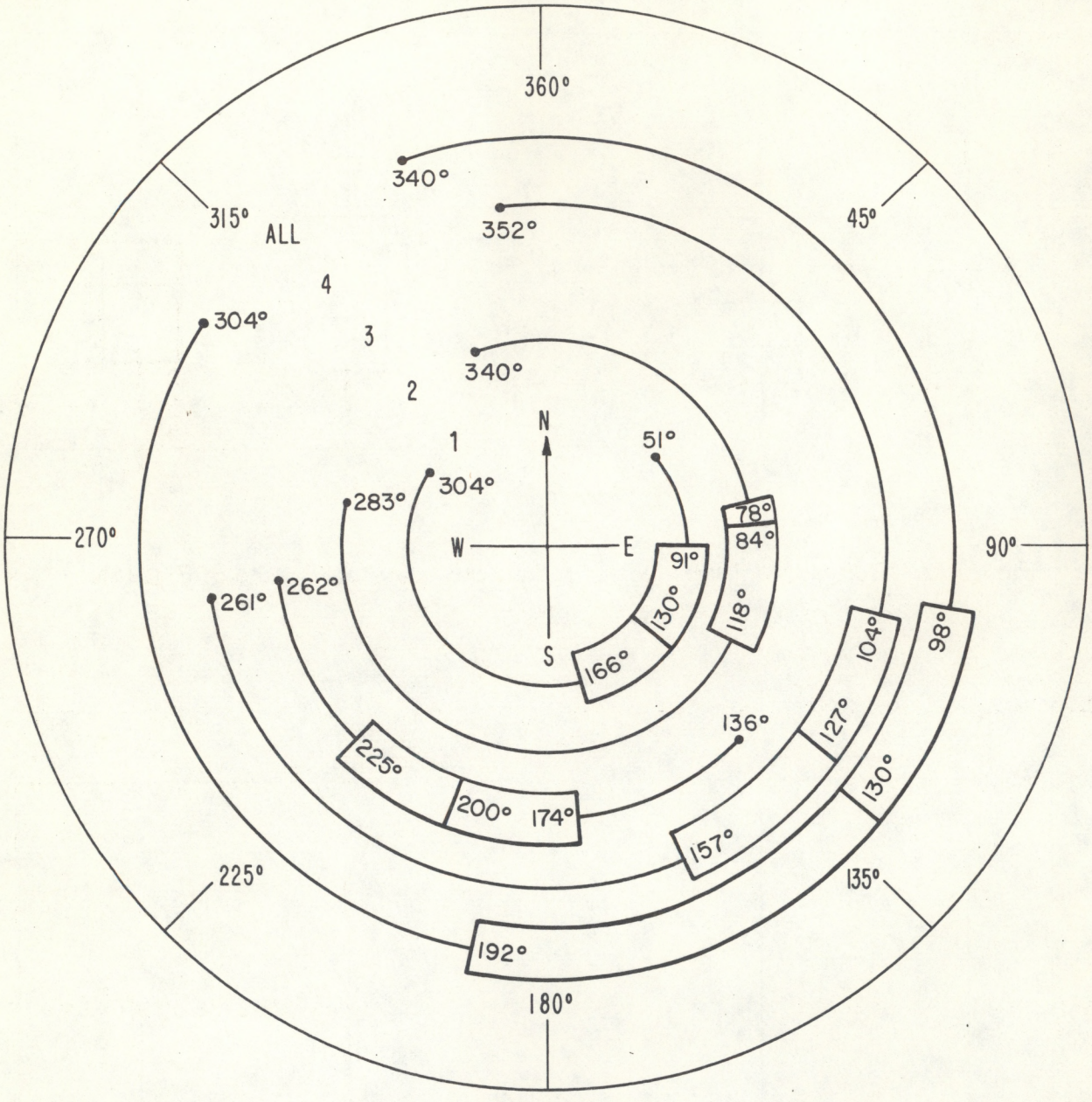

Figure 14. "Box-and-Whisker" plot of Mean Layer Vector Wind (MLVW) directions in polar coordinates (see legend of Fig. 11).

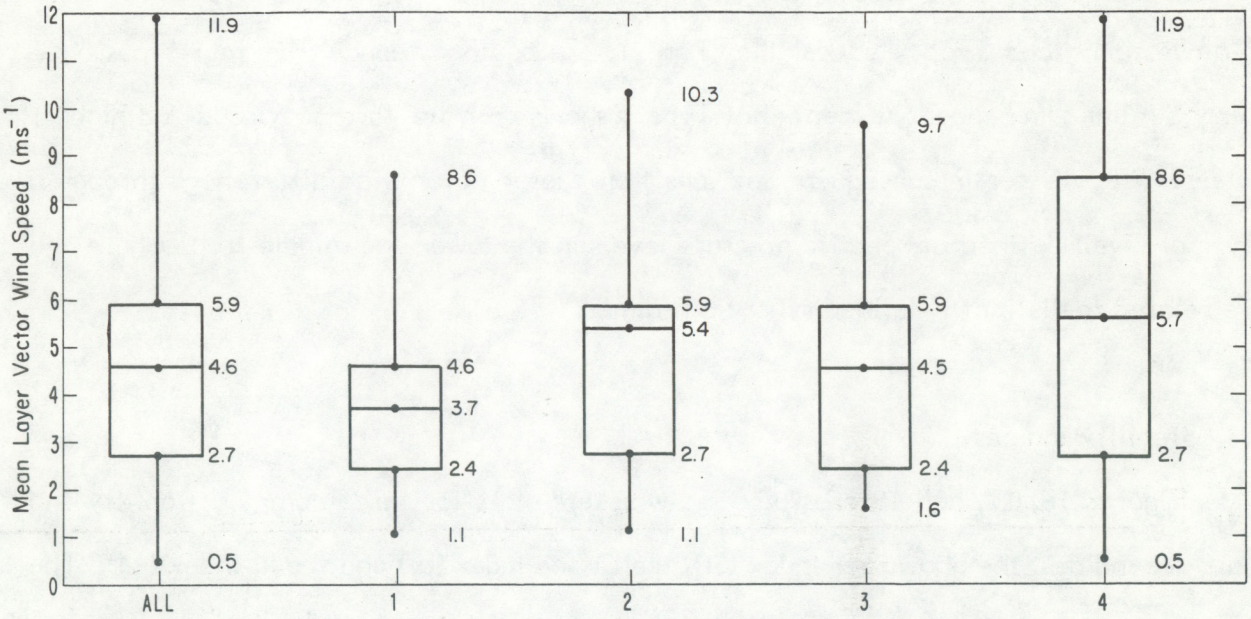

Figure 15. "Box-and-Whisker" plot of Mean Layer Vector Wind (MLVW) speeds (see legend of Fig. 11).

is shown in Section 4.6.1), there is little wind shear in this layer, and the MLVW is therefore a good representation of the low level wind.

If we look first at the wind directions, we see that there are distinct differences among the groups. Type 1 is typically dominated by a southeast wind through the lower portion of the troposphere; Type 2 winds are typically easterly; Type 3 winds are south-southwesterly; and Type 4 winds, like Type 1, are southeasterly. The four types have fairly similar wind speeds, except that Type 4 shows both the largest spread and highest values. We will see in subsequent sections that these vector wind differences through a layer are well defined at specific pressure levels in the lower and middle troposphere and are related to distinctly defined synoptic regimes.

4.5. Stability Indices

Figures 16, 17, and 18 are "box-and-whisker" plots for three common stability and moisture indices, the Showalter Index (SI), the Lifted Index (LI) and the K-Index (KI). The Showalter and Lifted Indexes yield a number that is proportional to the latent instability of the observed atmosphere by comparing the temperature of a parcel of low-level air after lifting to the 500-mb level with the temperature of the undisturbed environmental air at the same level. The temperature excess (deficit) is related to the size of the positive (negative) energy area on a thermodynamic chart.

To calculate the Lifted Index, the mean mixing ratio in the lower 915 m (3000 ft) of the sounding is determined by equal area averaging. Then the mean potential temperature in the lower 915 m at the time of convection is determined by forecasting the afternoon maximum temperature and assuming that a dry adiabatic lapse rate will prevail through this 915-m layer. (If significant heating or cooling is not expected during the afternoon, the mean temperature of the lower 915 m as shown in the sounding is used.) From these mean values the convective condensation level, or CCL, is located. Then the saturation adiabat through this CCL is extended upwards to 500 mb to find

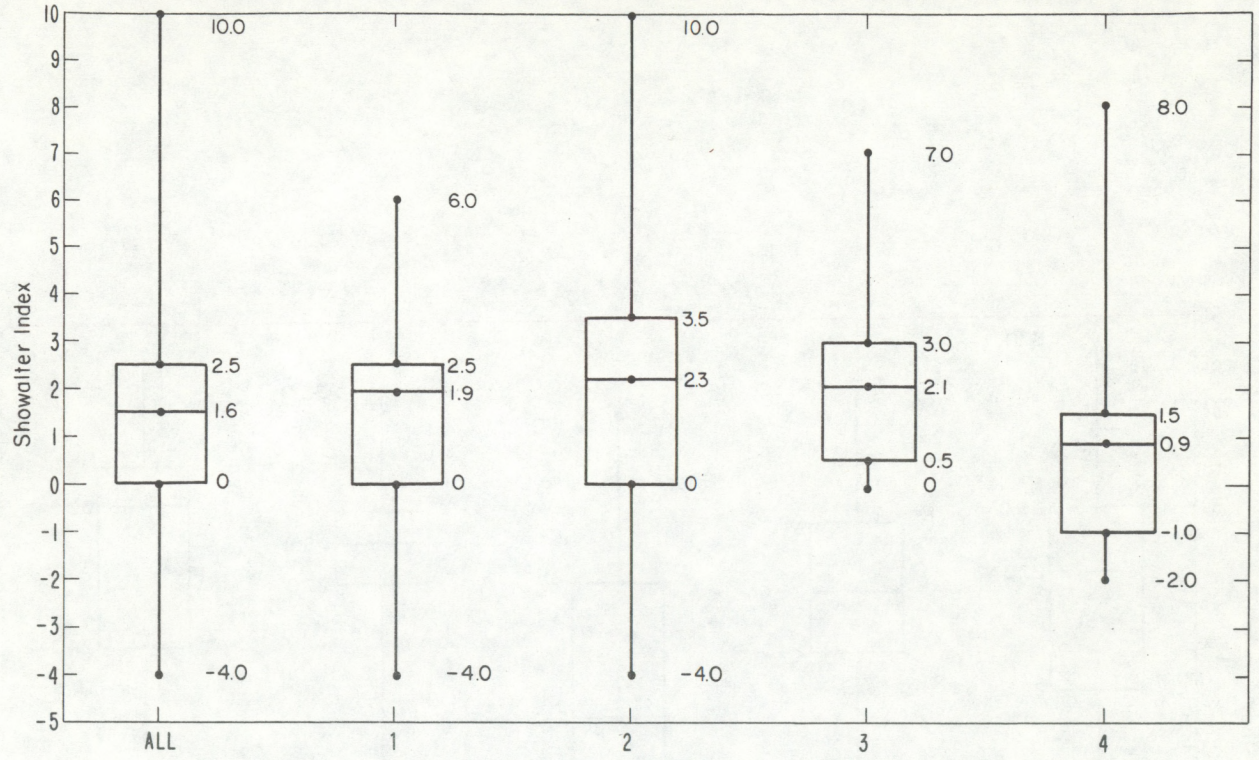

Figure 16. "Box-and-Whisker" plot of Showalter Index (see legend of Fig. 11).

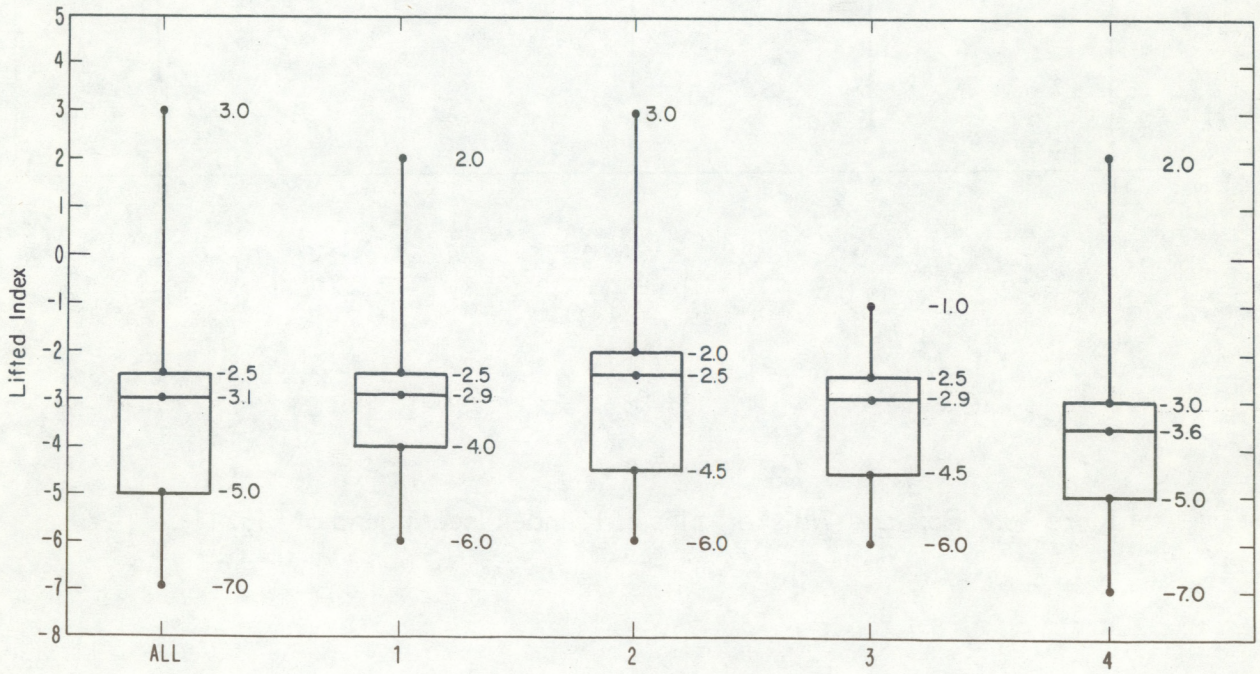

Figure 17. "Box-and-Whisker" plot of Lifted Index (see legend of Fig. 11).

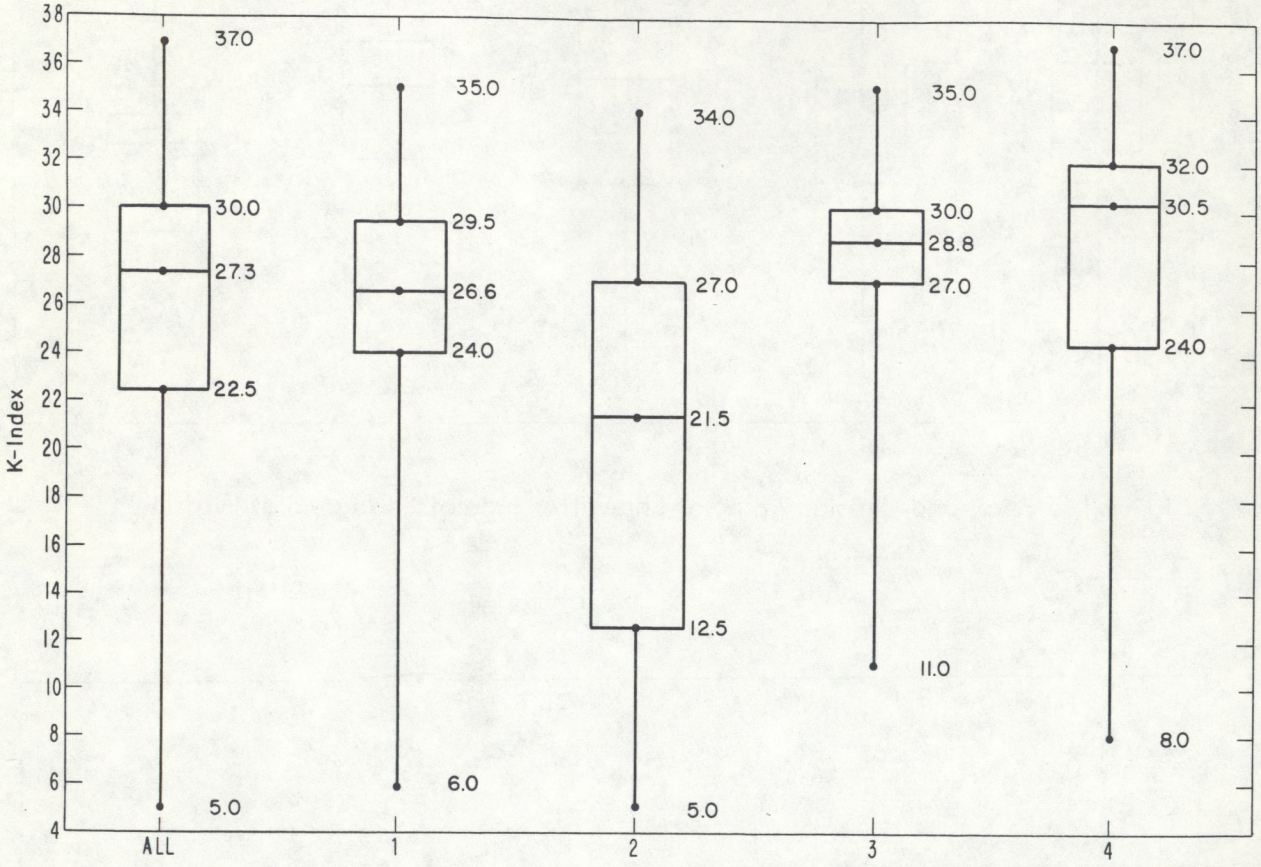

Figure 18. "Box-and-Whisker" plot of K-Index (see legend of Fig. 11).

T^*_{500}. The temperature of this parcel is subtracted from the environmental temperature at 500 mb to give the LI.

The SI is defined as the algebraic difference between T_{500} and T^*_{500}, where T_{500} is the environmental air temperature and T^*_{500} is the temperature of an air parcel that has been lifted adiabatically from 850 mb to 500 mb. The lifting process proceeds dry-adiabatically to the convective condensation level; then the parcel is lifted moist-adiabatically to 500 mb. Generally, the values are more positive than LI values, and as in the LI, greater stability is indicated by more positive (less negative) values.

The KI considers the overall static stability of the 850 to 500 mb layer by simply subtracting the observed 500 mb temperature from the 850 mb temperature, and it considers the positive contribution of high moisture at low levels by adding the 850 mb dewpoint temperature. The 700 mb dewpoint depression is used to account for possible buoyancy reductions due to the entrainment of dry environmental air. The computing formula is

$$K = (T_{850} - T_{500}) + T_{d\,850} - (T_{700} - T_{d\,700}) \qquad (2)$$

where T_d is the dewpoint temperature and the last term in brackets represents the dewpoint depression. As a general rule, convective activity becomes more widespread over south Florida as the KI increases.

If we examine the plots for these three indices (Fig. 16-18) we see that Type 4 has the least positive (most unstable) SI and LI, in addition to having the highest KI, all indicators of excessive convective activity. This is in agreement with the values previously shown for the rain volume and echo area coverage. Looking at Type 2, we see that the SI and LI exhibit the most positive (most stable) values of the four types, while having the lowest KI value, which is also in excellent agreement with the rainfall volume and echo area coverage. The observed convective patterns, it seems, are related to the

thermodynamic characteristics of the air mass located over south Florida, which is, in turn, controlled by the dynamic wind fields. These wind fields are discussed in detail in the next section.

4.6. Synoptic Characterization

As mentioned in earlier sections, each of the four convective pattern types is associated with a fairly distinct and easily distinguishable synoptic pattern. Not only is the flow field distinct, but, in addition, many of the thermodynamic characteristics are as well. This is to be expected since the thermodynamic structure of the atmosphere is closely linked to its dynamic state.

For the thermodynamic characteristics of the atmosphere, averaging was done only for the Miami (MIA) and West Palm Beach (PBI) radiosonde sites (which are treated as one site, as explained in Section 2.3); for the dynamic state of the regional atmosphere, ten radiosonde stations over the southeastern United States, the Bahamas, Cuba, and the West Indies were used. Winds, temperature, and moisture characteristics were analyzed at MIA and PBI since they are within the study area, but outside the study area, only winds were analyzed. The thermal and moisture characteristics at a station many hundreds of kilometers away may possibly have some effect on local convection. These effects might include the generation of gravity waves and their subsequent propagation into the region of south Florida where they could have an influence on local convection. Also, large areas of upward motion some distance away might result in local subsidence, thus preventing convection from taking place. A regional analysis of temperature, dewpoint, equivalent potential temperature, and mixing ratio at a number of pressure levels, however, showed no apparent pattern or relationship to the four convective pattern types. The winds then, as part of a larger scale dynamic feature, must surely play the dominant role in the initiation and organization of the peninsular-scale convection.

4.6.1. Single Station Results

Figures 19-23 show the mean sounding characteristics obtained from the combined MIA/PBI radiosonde data. No variances or standard deviations are shown because a much better understanding of the variability can be realized through the use of "box and whisker" plots (Figs. 11-18). Additionally, the computations of the mean wind directions and speeds were achieved through the use of u- and v-components, and it is not clear how one converts a variance of the u- and v-components into a variance for the wind direction and speed. The presentation used here is based on a similar presentation in López et al. (1983b).

Figures 19 and 20 depict the mean wind directions and speeds for the four types. These values were determined by computing the u- and v-components of each wind and then averaging the components. After averaging, the components were converted back into a direction and speed. Three facts are immediately apparent: 1) the directional shear between 950 mb and 400 mb is very small, 2) the wind direction is typically easterly (with the exception of Type 3), and 3) all the types have a northeasterly wind above about 350 mb. Type 2 days are distinctly more easterly to east-northeasterly, and Types 1 and 4 are southeasterly. Type 3 is generally southerly in the low levels and southwesterly in the middle levels.

A look at the mean wind speeds helps to distinguish further the differences (Fig. 20). Here, Types 1 and 4 are the two extremes of speed, whereas they were directionally very similar. Also, Types 2 and 3 are very similar in speed, but were directionally dissimilar.

The mixing ratio appears to be a good indicator of the similarities and differences of the thermodynamic state for the four types. Figure 21 is the mixing ratio difference for each of the four types. This difference is computed by finding the mean value for all days and then calculating the mean for each type and determining the difference

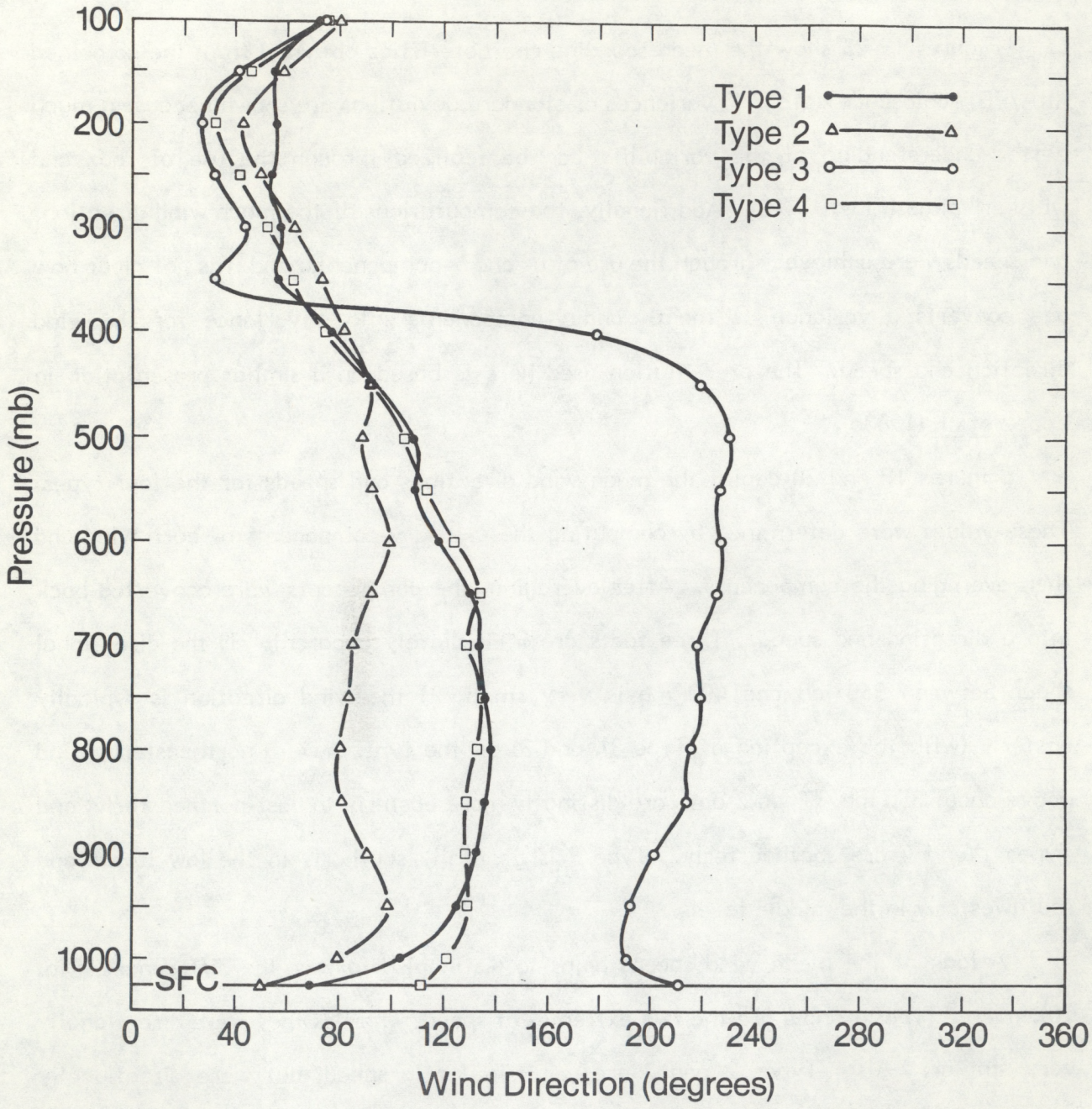

Figure 19. Mean wind directions at 50-mb intervals for each of the four convective pattern types.

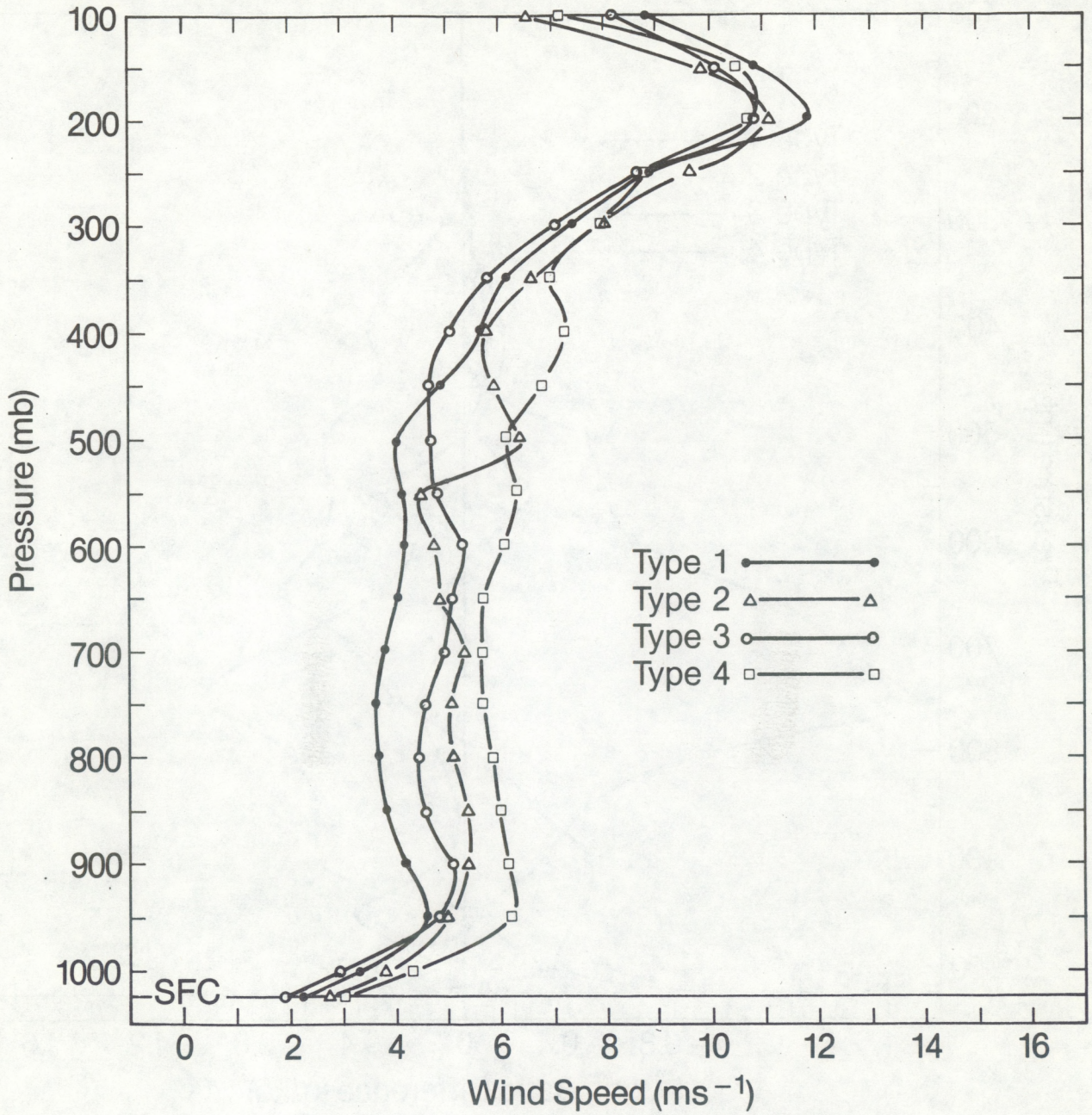

Figure 20. Mean wind speeds at 50-mb intervals for each of the four convective pattern types.

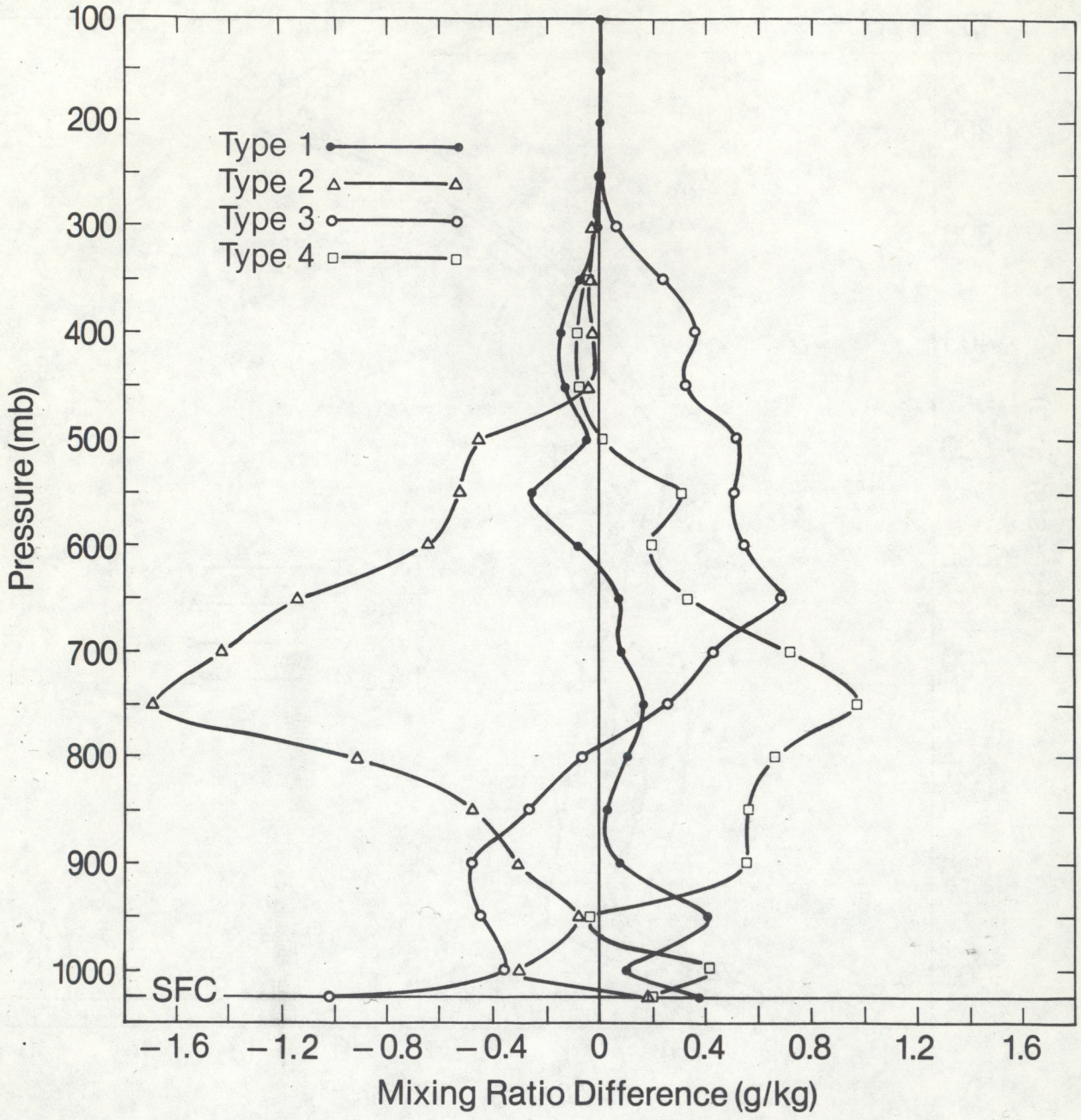

Figure 21. Mixing ratio differences at 50-mb intervals for each of the four convective pattern types. The difference is calculated from the mean of the days within a type and the mean of all the days together. Values greater (less) than zero indicate an excess (deficit) relative to the mean for all days.

between it and the mean of all days. In this figure, the mean of all the days is plotted along the zero line; moisture deficits and excesses are plotted to the left and right of the zero line.

Type I days show a slight excess from the surface up to about 650 mb, and a deficit above that level. The values of the excess and deficit are rather small, though. Type 2 days are the most extreme for this parameter. There is a slight excess in the lowest layers below 950 mb, but a large deficit from 950 mb to 400 mb; the maximum deficit occurs at 750 mb. This deep layer of relatively drier air helps to explain to a large degree the general lack of convection evident in the Type 2 radar figures. Type 3 days show slight deficits below 750 mb and somewhat larger excesses above that level. The Type 4 disturbed days exhibit small-to-moderate excesses at almost all levels below 500 mb, and have the largest excess in the middle layers, finally approximating the mean above 500 mb.

The wetter days, as determined by radar, all have moisture excesses in the middle troposphere; the drier days show moisture deficits in that same layer. Indeed, Frank and Smith (1968), Burpee (1979), and López et al. (1983b) all found that mid-tropospheric moisture was the single best predictor of precipitation and echo coverage for the Florida peninsula.

Figure 22 shows the temperature differences, derived in the same manner as the mixing ratio. At first glance, no apparent pattern emerges. Upon closer investigation though, certain interesting features are noted. Type I days show a profile that is not far removed from the mean, which is not unlike their mixing ratio profile. Type 2 days have a temperature deficit below 850 mb, an excess from 850 mb to about 450 mb, and a temperature deficit above this level. It is quickly obvious that this profile will produce a more stable lapse rate, which, in combination with its mixing ratio deficit, will tend to inhibit widespread convection. Type 3 days, on the other hand, show a temperature excess below 750 mb, a deficit from 750 mb to 500 mb, and an excess above 500 mb.

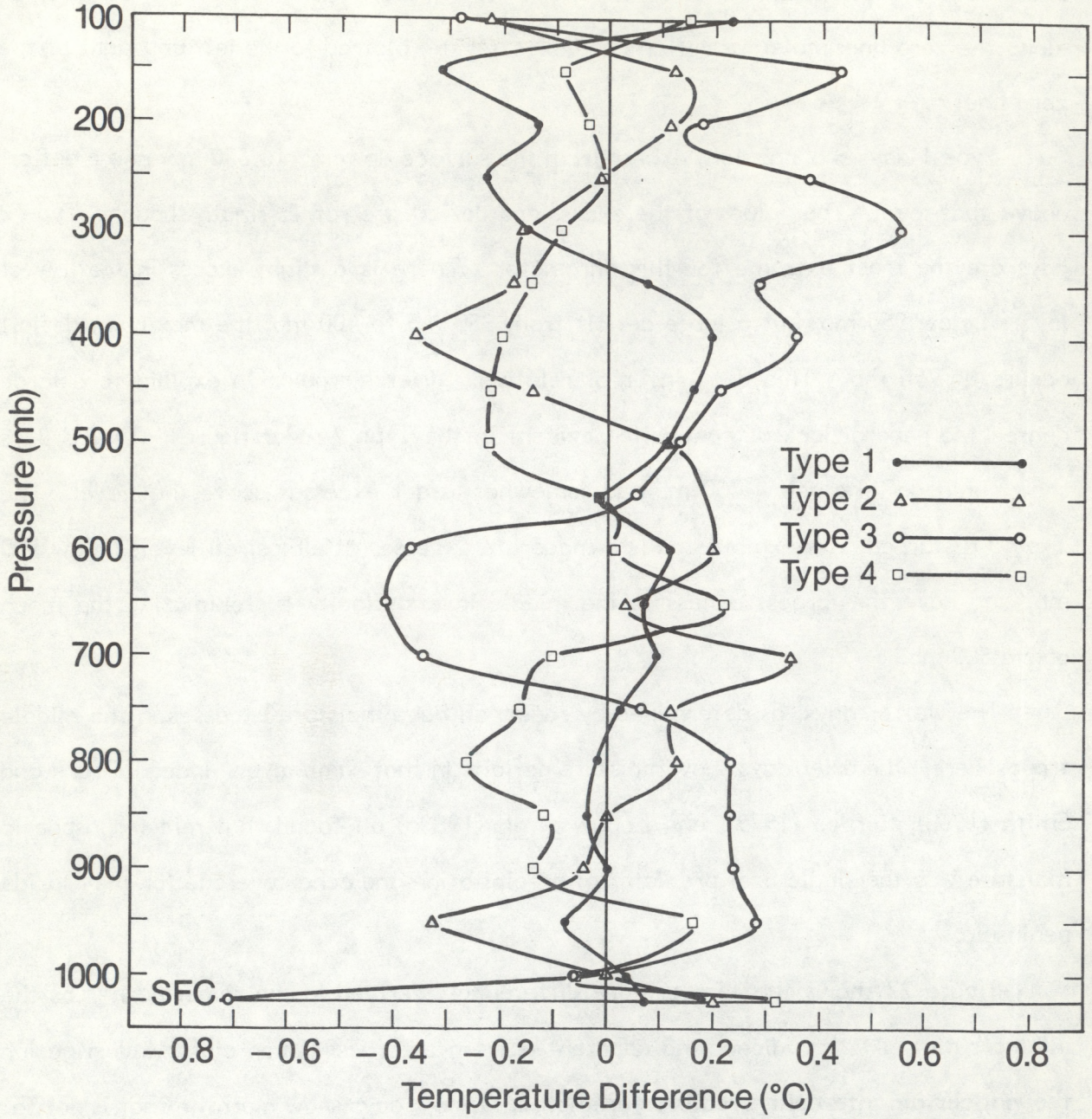

Figure 22. Temperature differences at 50-mb intervals for each of the four convective pattern types. The difference is calculated from the mean of the days within a type and the mean of all the days together. Values greater (less) than zero indicate an excess (deficit) relative to the mean for all days.

This combination will increase the instability, which, in turn, may be enhanced by its moisture excess (Fig. 21), resulting in a higher likelihood of widespread convection. Recall that Type 3 days did show a considerable amount of convection during the afternoon hours. Type 4 days show a slight temperature excess below 900 mb, a deficit from 900 mb to 700 mb, an excess from 700 mb to 550 mb, and a deficit above that. The instability is enhanced as in Type 3, but the transition from excess to deficit occurs at a higher pressure (lower height). This may partly explain why convection starts so early on these days. The greatest instability is fairly close to the ground, and only a small amount of solar insolation is needed to force an air parcel through the convective condensation level (CCL). Again, it should be pointed out that the differences between the types are small at most levels; nonetheless, the profiles make sense given the other information available.

Profiles of equivalent potential temperature (Fig. 23) are shown for each type at 50-mb intervals. The differences are small for all types at all levels except for a small layer from about 800 mb to 600 mb, and even here, only Type 2 shows any strong difference.

Reference has been made in the preceding paragraphs to the differences between means. A standard test of significance of the differences between means of groups is the t-test. This test, however, assumes that the data sample follows the normal distribution. Since most atmospheric parameters are not normally distributed, but rather are highly skewed, most of the standard parametric tests are inappropriate. A nonparametric test called Multi-Response Permutation Procedures (MRPP) is well suited to this type of data because it makes no assumption about the distribution of the population (Mielke et al. 1976, 1981). MRPP examines and compares the different data groups to determine whether they are from the same or different populations and gives the result in the form of a p-value of statistical significance. Typically, any p-value less than the 5% level allows rejection of the null hypothesis; i.e., that both groups of data

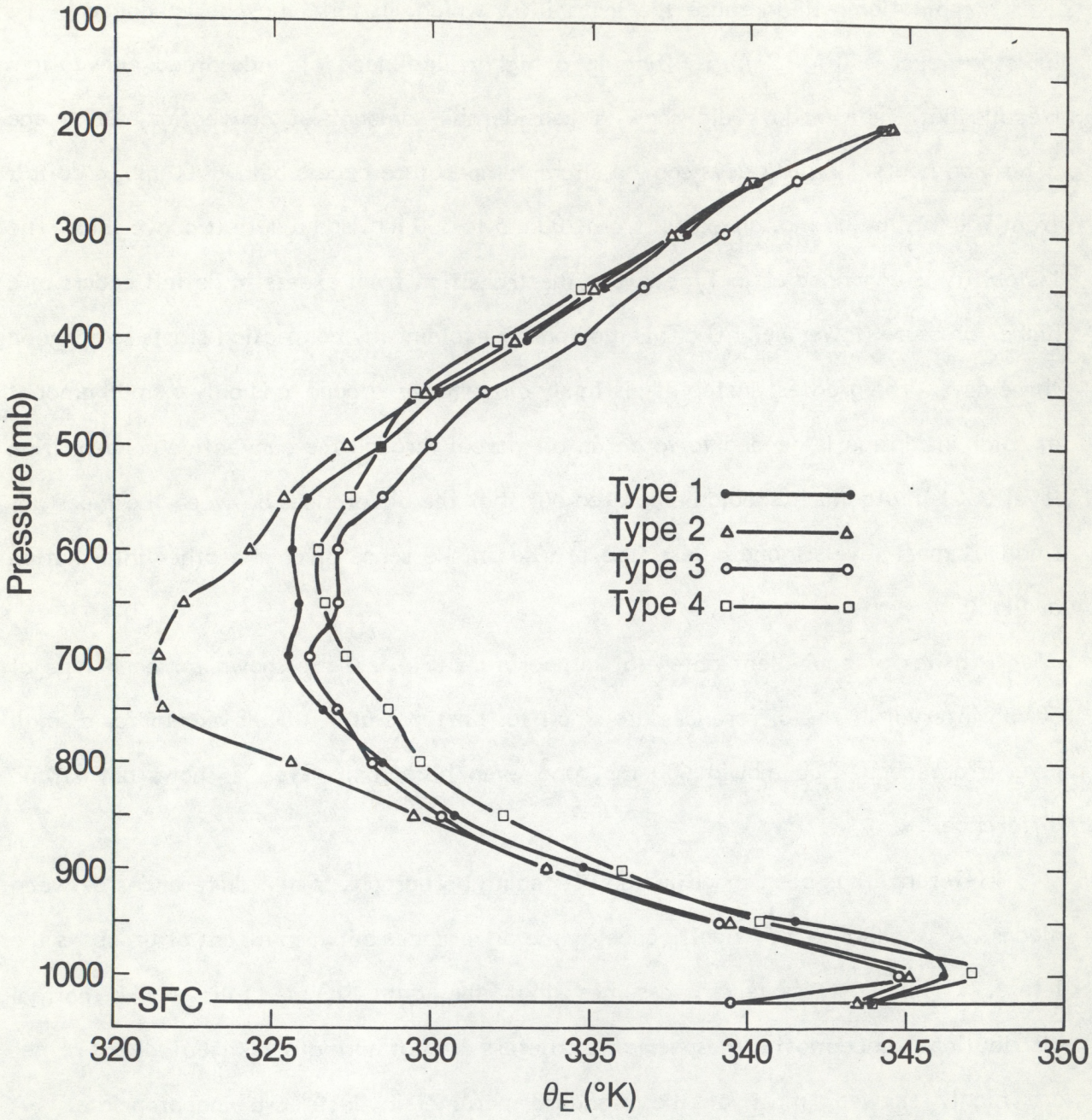

Figure 23. Mean equivalent potential temperatures at 50-mb intervals for each of the four convective pattern types.

are from the same population. An excellent description of this technique and its application to a simple meteorological problem can be found in Mielke et al. (1981).

To test all the variables at each available level would have been a monumental task, so only certain variables and combinations of variables were tested. The variables tested were the mean layer vector wind (MLVW); the temperature of the 500-, 700-, and 850-mb levels; a combination of the above; the three previously defined stability/moisture indices (i.e., the Lifted Index, the Showalter Index, and the K-Index); the K-Index alone; the radar-derived rain volume; and radar-observed echo area coverage. The reasons for these choices are straightforward. The MLVW can be quickly computed (or even estimated, if the wind shear is not large), and the temperatures at 500 mb, 700 mb, and 850 mb are routinely reported. The three indices are easily and routinely computed. The use of the K-Index alone was suggested by the relatively strong differences in Fig. 18. Thus, there are no difficulties associated with the computation of these selected variables. The last two (i.e. rain volume and echo area), were chosen to see if there were any differences, as detected by radar, that might be useful in distinguishing between the four types. The computed p-values for these combinations of variables are shown in Table 1.

The MLVW shows significant differences between the four types for all the six possible comparisons except between Type 2 and Type 4 (denoted hereafter as Types2/4). Recall from the earlier discussion that Type 2 and Type 4 were directionally dissimilar, but similar in speed. When these two parameters are combined back into a single vector variable however, these types are not distinctly different.

The temperatures at the three levels show little significance; p-values range from 16% to 66%. This is to be expected since Fig. 22 did not show strong differences.

The combination of the MLVW and temperatures gives mixed results relative to results for the MLVW alone. Two combinations show a slight improvement in p-values

(Types1/3 and Types2/4). The four remaining combinations, however, not only show no improvement, but go in the other direction with weaker p-values.

The combined stability indices are significant only for Types2/3, Types2/4, and Types3/4, and the K-Index alone is significant only for Types1/2, Types2/3 and Types 2/4. Recall that Type 2 days are very dry and Type 4 days very moist in the mid-troposphere, as shown in Fig. 21. That fact is reflected well here.

Table 1. Statistical significance of the differences between the means of groups; p-values are given for each of the six possible combinations. Values less than 5% ($.5X10^{-1}$) are considered significant and are underlined.

	P_{12}	P_{13}	P_{14}	P_{23}	P_{24}	P_{34}
MLVW	$\underline{.14X10^{-1}}$	$\underline{.19X10^{-5}}$	$\underline{.43X10^{-2}}$	$\underline{.18X10^{-3}}$	.25	$\underline{.20X10^{-2}}$
Temp.	.66	.28	.37	.16	.26	.24
MLVW/Temp.	.10	$\underline{.14X10^{-4}}$	$\underline{.28X10^{-1}}$	$\underline{.21X10^{-2}}$	.14	$\underline{.77X10^{-2}}$
KI/LI/SI	.16	.13	.18	$\underline{.31X10^{-2}}$	$\underline{.25X10^{-3}}$	$\underline{.31X10^{-1}}$
KI	$\underline{.24X10^{-2}}$	.21	.15	$\underline{.13X10^{-2}}$	$\underline{.45X10^{-3}}$	.27
Rain Volume	$\underline{.16X10^{-3}}$	.22	.22	$\underline{.34X10^{-3}}$	$\underline{.44X10^{-4}}$	.28
Echo Area	$\underline{.80X10^{-4}}$	.10	$.63X10^{-1}$	$\underline{.25X10^{-3}}$	$\underline{.11X10^{-5}}$	.11

The last variables are rain volume and echo area. Types1/2, Types2/3, and Types2/4 have small p-values, indicating significant differences between the means of the rain volumes. Types1/2, Types2/3, and Types2/4 again show strong p-values for echo area coverage; however, p-values for the remaining three combinations, although not

significant at the 5% level, are not far from it, indicating that these combinations, too, may represent different populations.

Summarizing Table 1, it is abundantly clear that the Type 2 days are quite different from the other groups. The four types show significant differences in some variables, but not in others. The MLVW seems to be the most important variable to consider when determining differences between the four types, since significant differences show up in five out of six combinations. Temperature appears to be of little use in determining differences between days, but the stability indices do well on three out of the six combinations.

4.6.2. Regional Scale Results

On the regional scale, the streamlines for some of the standard pressure levels were drawn by a modified Cressman (1958) scheme for the 1000-mb, 850-mb, 700-mb, 500-mb, and 200-mb levels. The stations used for this analysis are shown on the map in Fig. 24. The similarities and differences of the streamlines and the associated synoptic situation for each of the four types will be pointed out as well as their relationship to the convective patterns.

Type 1 days (Fig. 25) can be characterized as having a well-defined east-west ridge from the Atlantic Ocean extending over the peninsula. This ridge is the western extension of the regional scale Atlantic high, a semi-permanent feature over the Atlantic ocean in the summer. The position and strength of the ridge varies with time, owing to the passage of synoptic-scale systems in the westerly current to the north, or in the easterly current to the south. An important feature of Type 1 days is the termination of the ridge in the eastern Gulf of Mexico. This feature is especially evident at 1000 mb, 700 mb, and 500 mb. The breakdown of the ridge implies that the high pressure center is well away from the peninsula, or alternatively, is weak, or both. Regardless of the reason, the flow over the peninsula is fairly weak with anticyclonic curvature north of

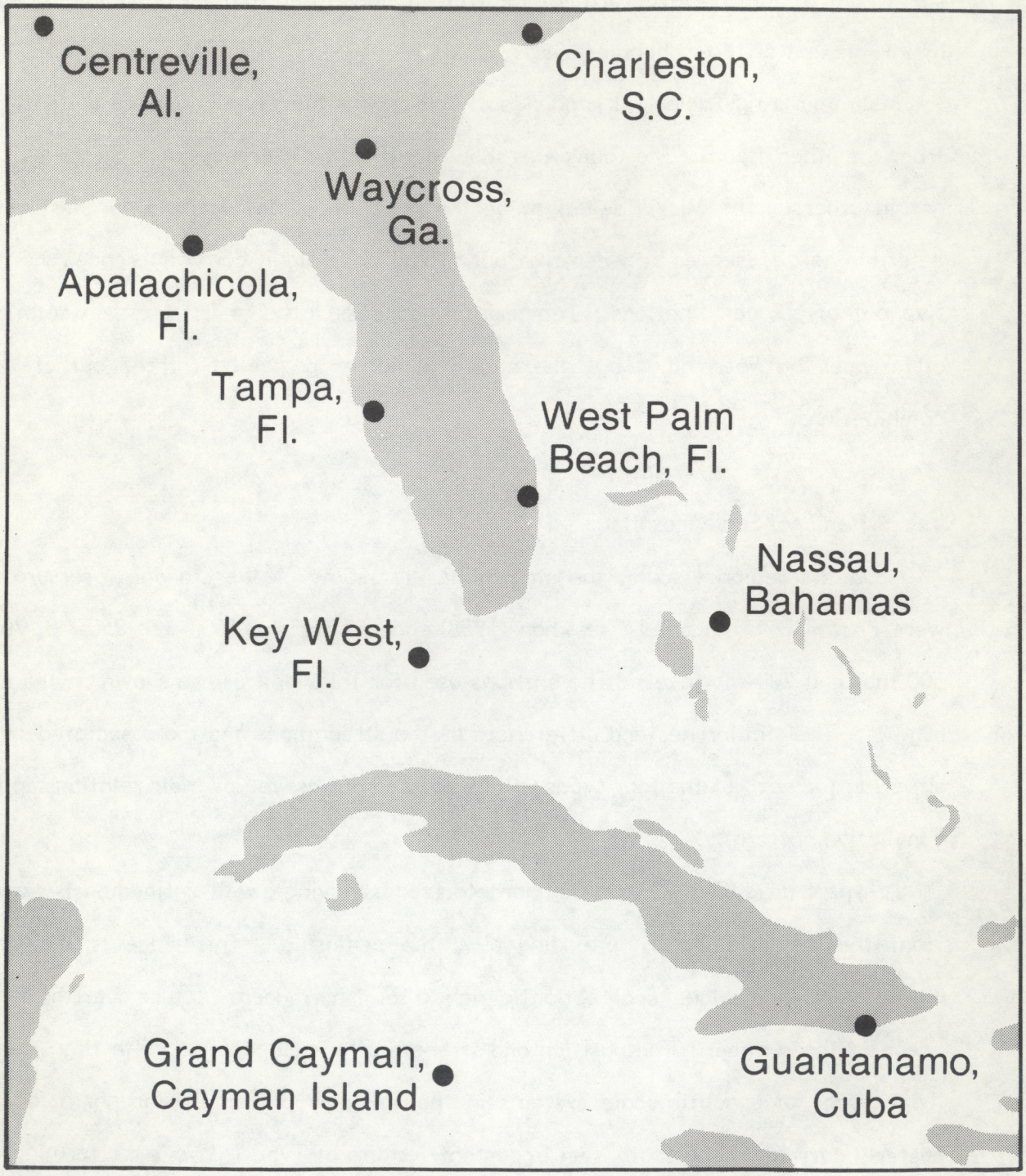

Figure 24. Map of the region showing the radiosonde stations used in the analysis.

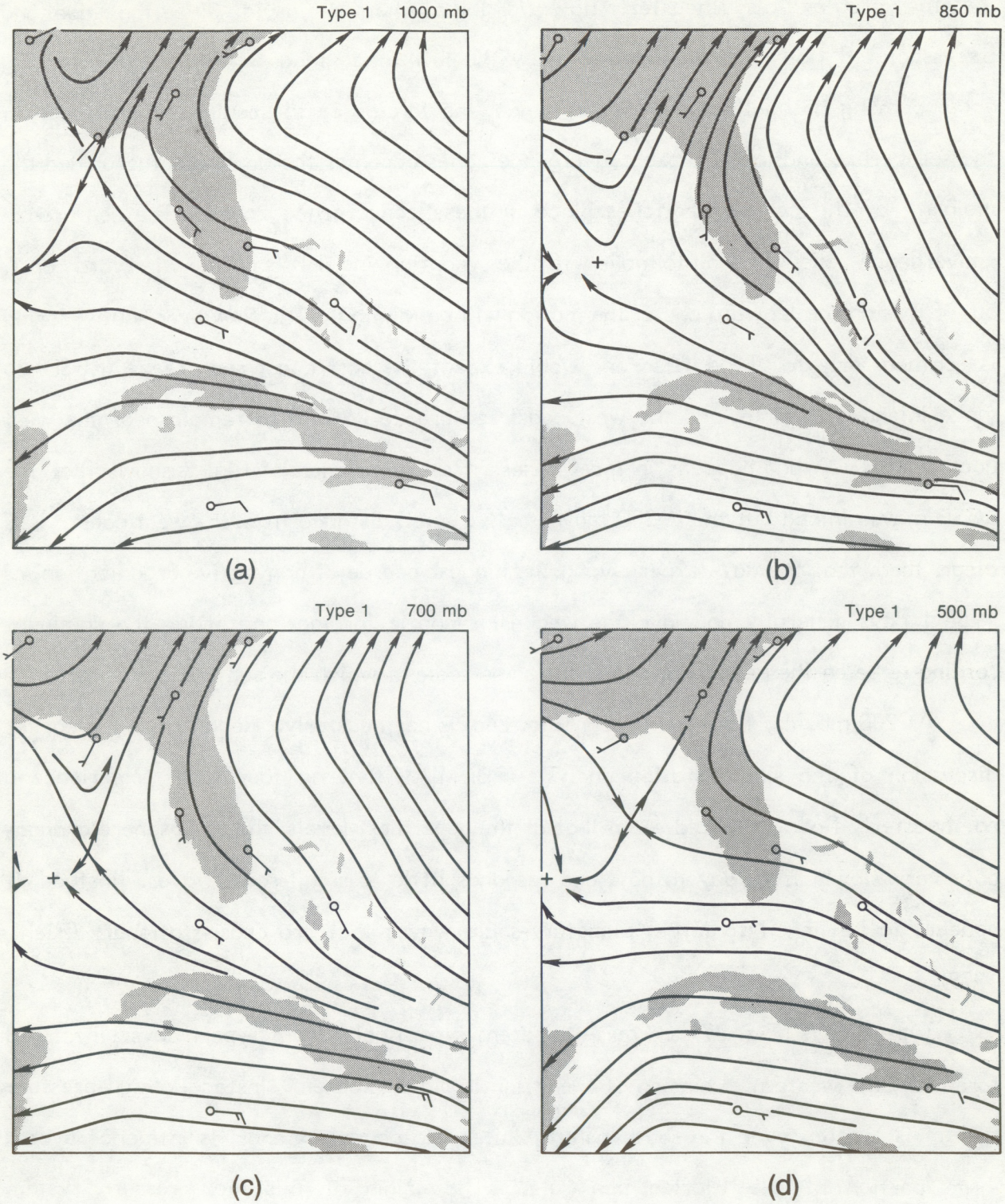

Figure 25. Mean synoptic wind field for Type I days at (a) 1000 mb, (b) 850 mb, (c) 700 mb, and (d) 500 mb. Full wind barbs are 5 ms^{-1}, and half barbs are 2.5 ms^{-1}.

the study area and a southeasterly flow over the southern peninsula. Since the ridge (and its associated flow) is weak, as shown by the low wind speeds in Fig. 25, the forcing accompanying it should also be weak; hence, the forcing on the peninsular scale due to the sea-breeze and lake-breeze convergence zones becomes the dominant factor and the majority of the convection takes place in these convergence zones. The sea-breeze convergence zone will tend to move with the synoptic wind if it is on the windward coast, but if it is on the leeward coast, the motion will be minimal. The flow over south Florida is southeasterly for Type I, so one would expect the east coast sea breeze (ECSB) to move inland with time, and the west coast sea breeze (WCSB) to remain near the west coast. This is what happens in most cases. Re-examination of Fig. 7 shows that the ECSB moves inland but the WCSB moves only a small distance from the west coast. It is clear, then, that the days experiencing the highest degree of convective organization, as Type I days generally do, have the weakest synoptic forcing, permitting the dominant forcing to be on the peninsular scale, the same scale at which the sea breeze operates.

At 200 mb, the flow for Type I (Fig. 26a) is northeasterly. Recall from the earlier discussion of the single station analysis (PBI/MIA), that all four types experience a northeasterly flow. It would seem that at the uppermost levels, the troposphere changes only very slowly from day to day, and responds little to small-scale waves. Instead, it appears to be linked to large, planetary-scale waves that are quasi-stationary (Riehl, 1979).

Type 2 days (Fig. 27) are quite different synoptically from Type I days. First and foremost, the western extension of the Atlantic ridge is absent. Instead, a high-pressure system is located over the southeastern United States and extends its influence over a large portion of the Florida peninsula. The origin of this high-pressure system (determined from an analysis of daily synoptic charts) is over the continental United States. There are warm temperatures through a deep layer due primarily to large-scale subsidence, and low humidities due partially to subsidence but also to the lack of a large

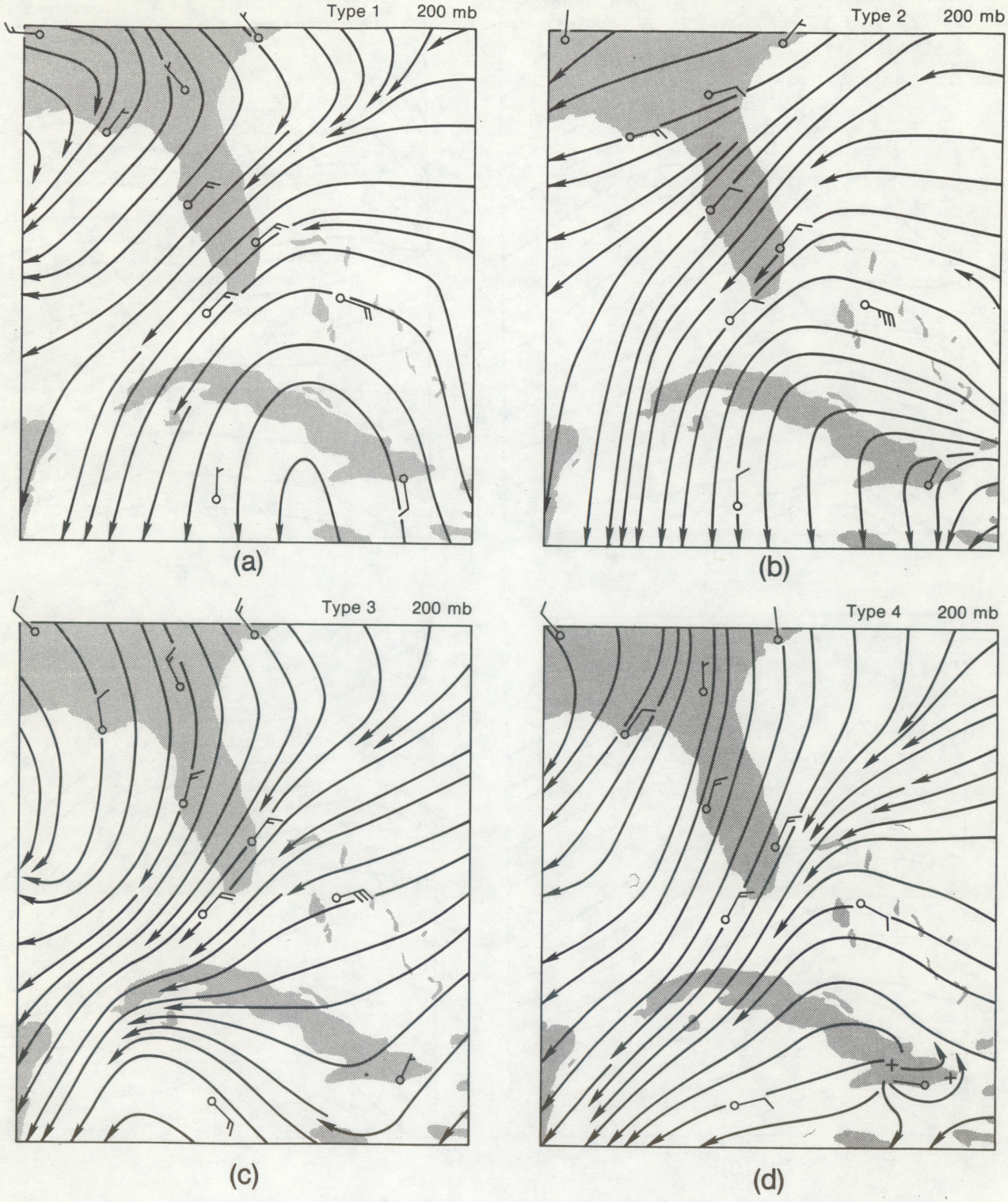

Figure 26. Mean synoptic wind field at 200 mb for (a) Type 1, (b) Type 2, (c) Type 3, and (d) Type 4 days. Full wind barbs are 5 ms^{-1}, and half barbs are 2.5 ms^{-1}.

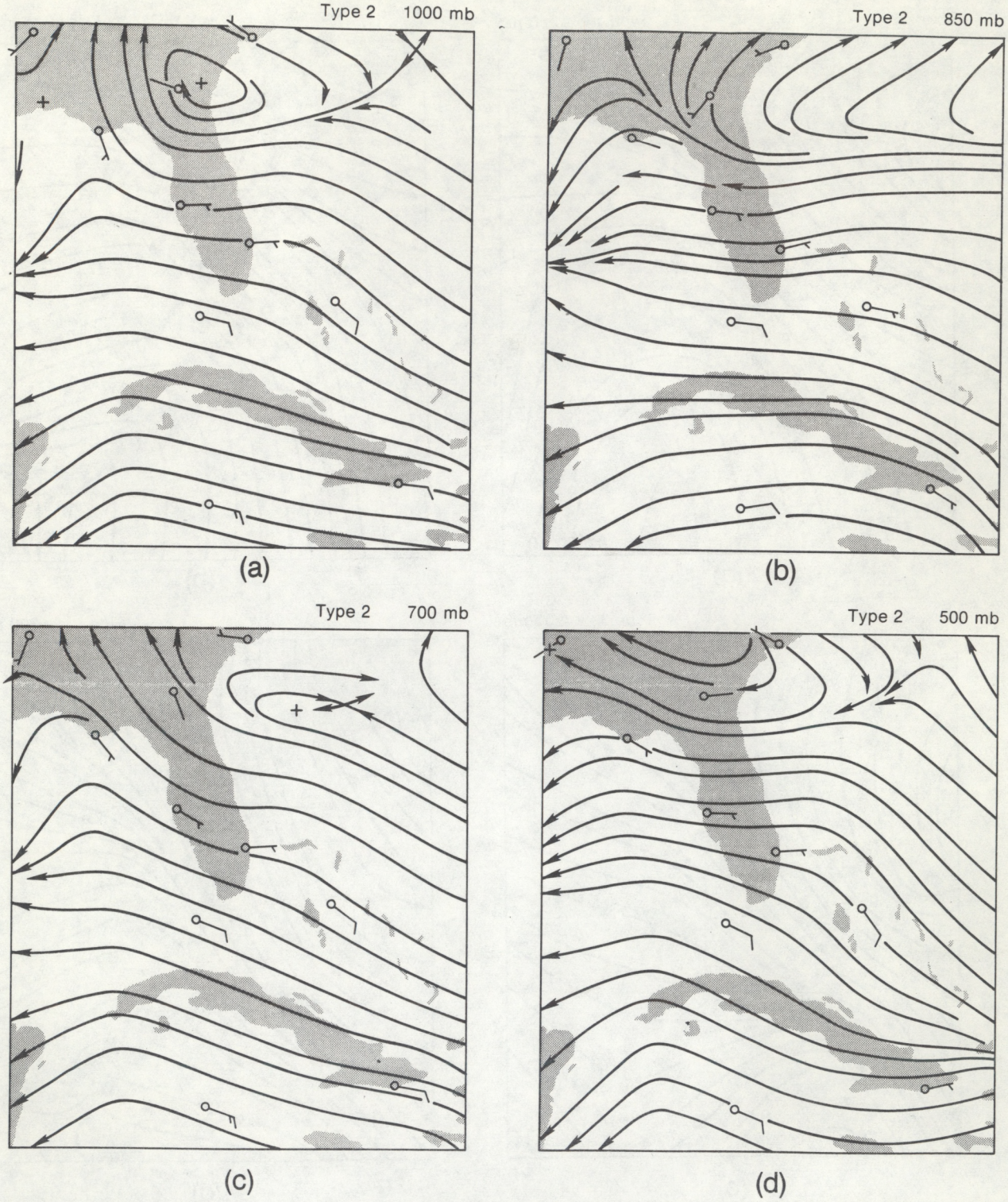

Figure 27. Mean synoptic wind field for Type 2 days at (a) 1000 mb, (b) 850 mb, (c) 700 mb, and (d) 500 mb. Full wind barbs are 5 ms^{-1}, and half barbs are 2.5 ms^{-1}.

underlying water body in the original location of the high. Typically, the high pressure system will form over the continent and move slowly to the east or southeast until it reaches the Atlantic Ocean. As the system moves out over the ocean, the air mass experiences a slow modification from the bottom up, particularly in the moisture. After some period of time, the high-pressure system has modified sufficiently so that its characteristics are not discernibly different from those of the Atlantic high and the two systems begin to blend into one, eventually reverting to a southeast flow over the peninsula and a ridge to the north.

Because of the thermodynamic characteristics of the continental high-pressure system, convection is sparse. Stable lapse rates and low moisture values discourage convection. It takes a considerable amount of forcing to set off convection, and the ECSB and WCSB are generally insufficient to do so. Only when the ECSB has moved to the west coast - and this is accomplished fairly easily since the synoptic-scale wind is oriented normal to the sea breeze - and merged with the WCSB, is the forcing sufficient to generate convection. This merger concentrates what little moisture and vertical velocity there is into a fairly small region. Also, curvature effects of the coastline enhance the sea-breeze forcing (Neumann, 1951; McPherson, 1970; Smith, 1970; Pielke, 1974). The major areas of convection, then, should be on the west coast where convex curvature effects enhance the convergence. Convection is sparse (see Fig. 8), and only when the ECSB has merged with the WCSB does it start to intensify and become more widespread developing a major area of convection in the region of strongest convex coastline curvature. As before, the 200-mb pattern (Fig. 26b) is northeasterly and bears only slight resemblance to the synoptic features located below it.

Since Type 3 is markedly different in its convective patterns from Types 1 and 2, one would expect the synoptic pattern to be equally different and, in fact, it is. Fig. 28 shows the typical synoptic situation associated with Type 3 convection. The Atlantic ridge is south of the study area, resulting in a south to southwest flow over the southern

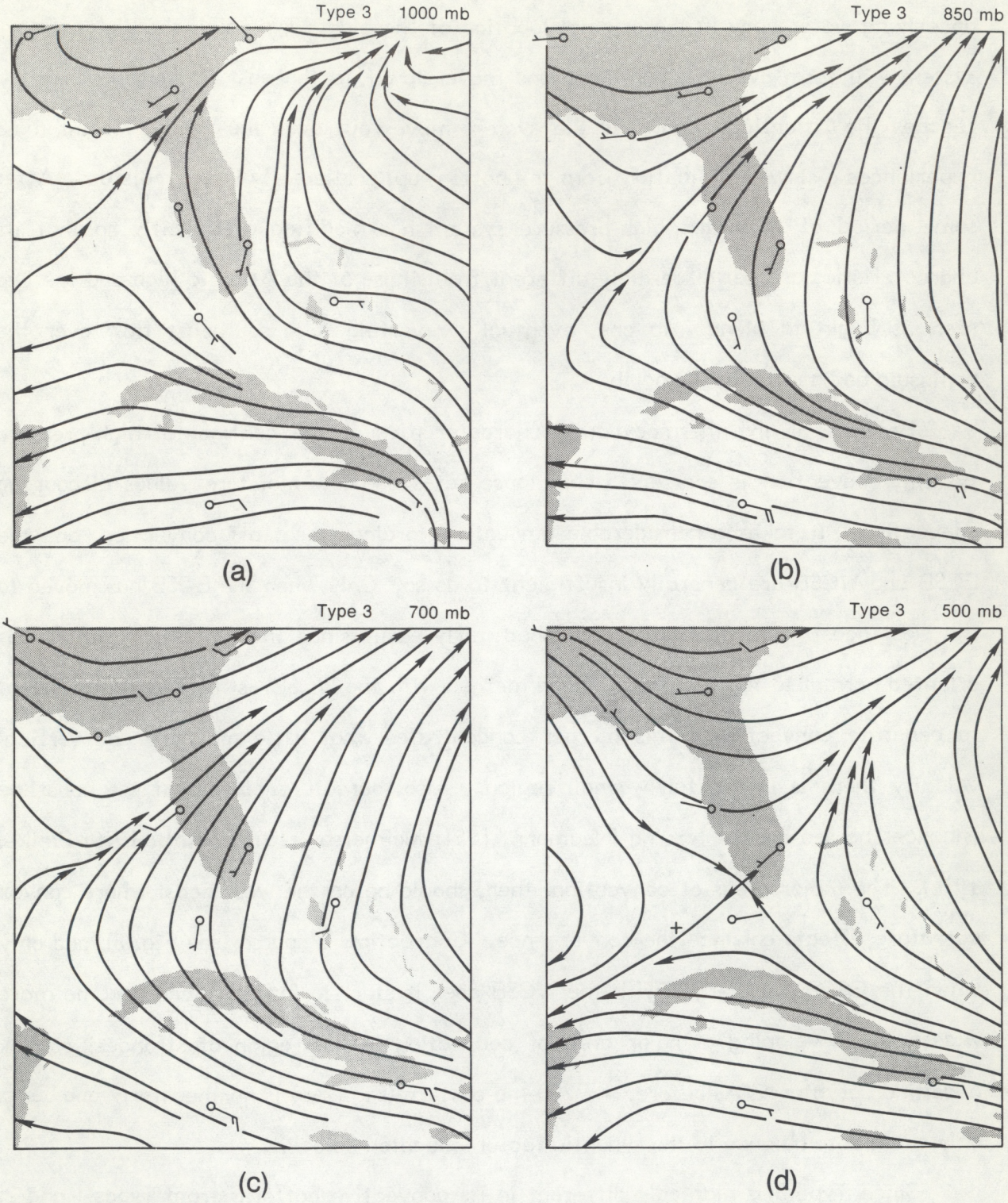

Figure 28. Mean synoptic wind field for Type 3 days at (a) 1000 mb, (b) 850 mb, (c) 700 mb, and (d) 500 mb. Full wind barbs are 5 ms^{-1}, and half barbs are 2.5 ms^{-1}.

part of the peninsula. Additionally, a short wave is evident, especially at 700 mb and 500 mb, to the north of the state of Florida. The eastward motion of this wave and its cyclonic flow field will result in increasing vorticity and vertical wind shear over the peninsula. On the synoptic scale, there will be vertical lifting (Holton, 1979). Note, also, the confluence zone over north Florida at 1000 mb, and over successively more southerly (albeit weaker) positions at 850 mb, 700 mb, and 500 mb. This pattern suggests that there will be sufficient synoptic-scale forcing due to convergence to trigger widespread convection. The large-scale lifting will contribute to destabilizing the atmosphere as a whole over the region, and the southwest flow will advect the windward (west coast) sea breeze inland while the leeward (east coast) sea breeze remains along the coast. It is important to remember that although there will be forcing at the peninsular (sea-breeze) scale, it will be modified by the synoptic-scale forcing. This is why Type 3 days are not simply a reversed version of the Type 1 days. As with Type 1 and Type 2 days, the 200-mb pattern for Type 3 days (Fig. 26c) shows northeasterly flow over the peninsula and bears little resemblance to the patterns beneath it.

Earlier it was shown that from a single station (PBI/MIA), Type 1 days and Type 4 days were directionally very similar, although their wind speeds represented the two extremes. Figure 29 shows quite clearly that the synoptic pattern for the Type 4 days is markedly different from that of Type 1 days. Type 1 days, it will be recalled, showed a well-defined ridge extending westward over Florida and terminating over the Gulf of Mexico. Type 4 days do not have any ridge over the peninsula. A ridge is (possibly) present at the northern boundary of the region. The major difference between the types appears to be the location of the ridge. In the configuration shown here, the air passing over Florida is being advected out of the deep tropics and has thermal and moisture characteristics typical of that region; that is, there is a fairly deep layer of moisture present in a convectively unstable column. Although not evident at 1000 mb, and only slightly evident at 850 mb, a reasonably well-defined easterly wave can be seen at 700

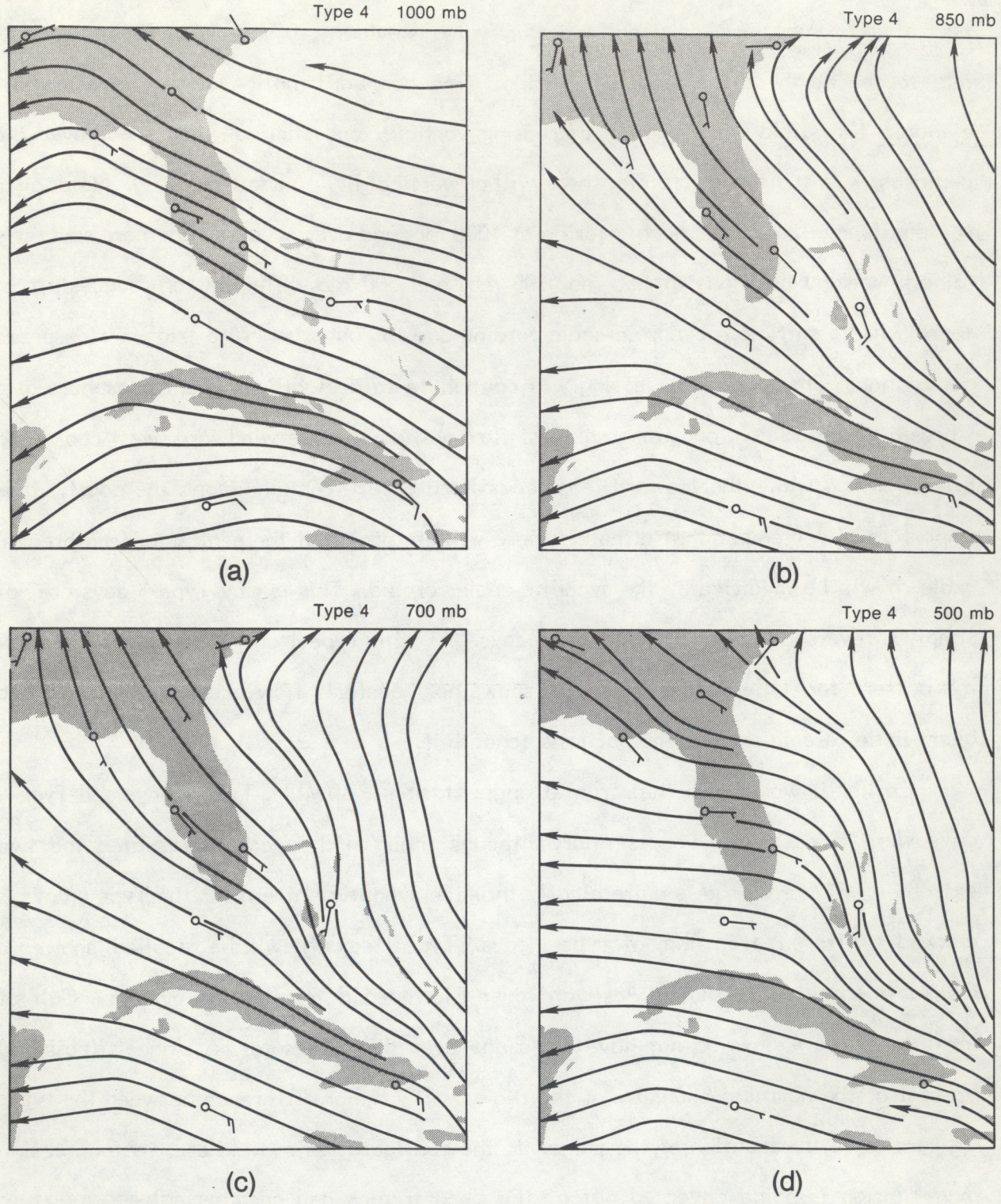

Figure 29. Mean synoptic wind field for Type 4 days at (a) 1000 mb, (b) 850 mb, (c) 700 mb, and (d) 500 mb. Full wind barbs are 5 ms^{-1}, and half barbs are 2.5 ms^{-1}.

mb and 500 mb to the east of the Florida peninsula. This is just one of the tropical-type disturbances mentioned earlier. Also, there is a feature evident at 200 mb (Fig. 26d) that is not present in the other three types. Although the flow is still northeasterly over Florida, there is a trough to the east, in which a closed cyclonic circulation will often be present. Because of the scarcity of data for this region, the objective analysis scheme cannot determine well enough the location or shape of this circulation; nonetheless, the analysis and data suggest the existence of a circulation of sorts. These "cold lows" (Palmén, 1949; Carlson, 1967; Frank, 1970; Kelly and Mock, 1982) are strongest at 200 mb, but often exert their influence down to 500 mb. The cold temperatures aloft destabilize the atmosphere, and the circulations often have regions of divergence ahead of them. The combination of these two factors promotes widespread convective activity over south Florida and the adjacent waters.

In general, it can be seen that the two principal features determining the large-scale flow over south Florida during the summer are (1) the position and strength of the Atlantic high-pressure region and its relationship to the peninsula, and (2) the passage of tropical or middle-latitude disturbances. The first determines how much suppression exists over the region; the second, how much enhancement of the diurnal (sea-breeze-induced) convection is present.

4.7 Further Discussion

The foregoing results make it very clear that the patterns of convective activity on a given day are controlled principally by the large-scale dynamics and subsequently by the thermodynamics typical of the synoptic pattern. These, of course, are not the only factors that control convection. Surface features, it was pointed out, such as Lake Okeechobee, the water conservation area, and the swamps inhibit convection; coastline curvature effects, and certain types of surface vegetation and soil, may promote convection.

Wiggert and Lockett (1981), using the same radar data as those used here, looked at the characteristics of individual radar cells over their lifetime. They found that the radar echoes had larger than average areas and volumetric rain rates if they were stationary or embedded in light, low-level winds. López et al. (1983a,b) also found that, in general, the degree of convective activity increases as the wind speed decreases. Those results at first seem to disagree with the findings of this study. Recall that the Type 1 days had the slowest wind speeds, followed by Type 3, Type 2, and finally Type 4. Also recall that the Type 1 days were the most organized of all the types but produced only the third-wettest days, and Type 4 days were both the wettest and had the strongest winds. The answer to this seeming contradiction is twofold. First and foremost, Wiggert and Lockett (1981) and López et al. (1983a) looked at only those days that were determined to be neither suppressed nor disturbed. Therefore, they were looking primarily at variations of convection within one or two of the types discussed in this study. Second, the previously mentioned studies dealt with individual radar echoes. On that scale, their findings appear to be correct; however, it cannot be overlooked that if a larger scale phenomenon is controlling the convection over the peninsula, the total number of echoes may be increased manyfold, so that even though they may individually produce less precipitation as detected by radar, collectively they produce more over the entire region.

It is easily seen that the convective patterns (Figs. 7-10) are best defined in the early part of the day, and become somewhat obscured with time. Cooper et al. (1982), in a study of convection and forcing over south Florida, looked at a number of different scales and their interaction. They found that by taking the time derivative of the convergence curve shown by Frank et al. (1967) they could determine the peninsular-scale forcing, or vertical acceleration. Additionally, they used convergence values from a smaller network to look at scales on the order of individual storms. They found that the maximum value of the ratio of upward convective transports to downward convective

transports occurred at roughly the same time as the maximum peninsular-scale forcing near 1230 EDT. The peninsular-scale forcing drops off rapidly afterwards and eventually becomes negative. The upward and downward convective transports continue on for a number of hours until they too begin to dissipate. Cooper et al. suggest that in the early part of the day, convection and its organization are initiated by the peninsular-scale forcing, which is, in turn, under the control of the synoptic flow. As this force weakens, the primary forcing is due to the convergence/divergence associated with individual updrafts and downdrafts on the convective scale. Thus, new convection and its organization are partially determined by this convective-scale forcing; however, the new convection will preferentially occur in those regions where the peninsular-scale sea breeze has already concentrated the heat and moisture. Many other investigators, including Simpson (1980), Simpson et al. (1980), Cunning and DeMaria (1981), Cunning et al. (1982), Holle and Maier (1980), and Purdom (1979), have noted that new cloud growth over south Florida is intricately tied into downdraft interaction with the ambient wind field. Finally, Cooper et al. (1982) went on to say that they believed nowcasting of convection in south Florida was possible, given the synoptic situation that starts the process, and knowing the surface layer velocity fields once the process is going.

5. SUMMARY AND CONCLUSIONS

The findings of previous investigators, including Byers and Rodebush (1948), Day (1953), Gentry and Moore (1954), Frank et al. (1967), Frank and Smith (1968), and Smith (1970) helped lay the groundwork for the study and understanding of Florida cumulus convection. Building upon these observational studies were the numerical studies of Estoque (1962), Pielke (1974), Pielke and Mahrer (1978), Gannon (1978) and McCumber (1980). All of these numerical studies have portrayed quite well the convection and how it is linked to many different interacting scales and is modified by land, vegetation, and soil features. The present study has built upon the previous investigations in order to realize better the variations of convection over the south Florida peninsula through the use of a data set with very high spatial and temporal resolution. This data set makes it possible to determine the small-scale spatial variations of convection as well as short-term temporal variations. For the purposes of this study, the spatial resolution was essentially maintained - modified only to the extent of transforming polar coordinate data into Cartesian coordinates. Temporally, however, the data were degraded from the original resolution of one full radar scan every 5 minutes to an averaged scan every 3 hours. This was necessary because, first and foremost, the volume of the original data would overwhelm the study. Second, the idea was to gain an understanding of the basic patterns prevalent within a type of day and the 3-hour data appear to be adequate for this purpose. López et al. (1983b), using this same data, approached the study of south Florida convection from a different perspective. They maintained the temporal resolution of one scan every 5 minutes at the expense of degrading the spatial resolution by converting the space domain into a single area-wide value for the parameters

studied. Their study is, of course, the companion to this one. By integrating the spatial and temporal results of these two investigations, it is possible to gain a great deal of insight into the dynamics and kinematics of cumulus convection over south Florida during the summer.

It has been shown in this paper that four basic convective pattern types are observed over south Florida during the summer months. Within any one type there may be numerous variants, but, in general, the variations within a type are far smaller than the variations between types.

Type 1 days have well-defined sea-breeze convergence zones located on each coast. The east coast sea-breeze (ECSB) convergence zone propagates inland while the west coast sea-breeze (WCSB) convergence zone remains close to the coast. By late in the afternoon, there is a merger of the two sea breezes to the west of the center of the peninsula. The resultant convection is often stronger and longer-lived than that of either sea breeze alone. Convection usually dissipates during the early evening.

Type 2 days are quite dry and the sea breezes are usually insufficient to generate more than isolated convection. The ECSB moves quickly to the west coast where it merges with the WCSB. Convection begins to increase within this merged region. Enhancement is noted in areas where there is convex curvature of the coastline; the opposite occurrs in areas where the coastline has a concave curvature. The convection usually is advected westward into the Gulf of Mexico by the prevailing synoptic-scale winds.

Type 3 days start fairly quickly on both coasts. The WCSB moves inland and overtakes the ECSB; then the merged area moves offshore with the prevailing winds. The area covered by radar echo is typically greater on Type 3 days than on Type 1 or Type 2 days. Additionally, convection does not dissipate as early on Type 3 days.

Type 4 is a mixed group of disturbed days, whose disturbances are both easterly (easterly waves, upper tropospheric cold lows) and westerly (middle-latitude westerly

waves, dissipating cold fronts), and days that have a deep layer of very tropical air being advected straight out of the tropics. Convection starts early in the day, very quickly spreads to cover large areas of the peninsula, and is slow to dissipate in the evening.

The convective patterns are controlled to a large degree by the synoptic-scale flow. This large-scale flow is the result of the placement and strength of the Atlantic high-pressure system, which is constantly undergoing modification because of the passage of waves in both the westerly current to the north of its center and ridge axis which extends to the west, and in the easterly current to the south. Additionally, there may be variations of the location of the center of the system and its domain of influence. All of these factors play a major role in determining the direction and speed of the regional- and synoptic-scale winds over south Florida. These winds, in turn, control the development and organization, but not necessarily the strength (Burpee, 1979), of the forcing of the sea breezes along the east and west coasts of south Florida. It is within the convergence zones associated with the sea breezes that the majority of convection develops, although not all the convergence zone experiences convection on any given day (Pielke and Mahrer, 1978). The windward coast sea breeze moves inland with time while the leeward coast sea breeze remains anchored along the coast or moves inland only very slowly on days when the synoptic winds are not too strong. On days with stronger winds, the leeward sea breeze will probably be advected offshore during the course of the afternoon. Disturbed days usually produce an abundance of convection, yet the sea breezes are still present, although they have a reduced role in the production of peninsular precipitation. Suppressed days, obviously, have a lack of convection, yet the convection that is present is more often that not located within one or both of the sea-breeze convergence zones or the lake-breeze convergence zone.

The thermodynamic properties of the atmosphere, as sampled by the radiosonde sites at Miami (MIA) and West Palm Beach (PBI), (and treated as a single station), exhibit differences from one type to the next. Not all the differences can be shown to be

statistically significant using the nonparametric MRPP test techniques (Mielke et al., 1976; 1981), but the differences, relative to the other types, appear to be consistent in the sense of warmer or cooler, drier or wetter.

Further modifications of the patterns appear to be either a direct or indirect consequence of the variations of surface features. Large bodies of water tend to inhibit or weaken convection, and certain combinations of soil and vegetation appear to enhance convection. Also, the curvature of the coastline, especially that of the southwest coast of Florida, can either concentrate or dilute the effects of convergence resulting in an enhancement or weakening of convection in those regions (Neumann, 1951; McPherson, 1970; Smith, 1970; Pielke, 1974).

Interactions on the scale of the cumulus convection itself can play an important role in the evolution of the convective pattern an any day. Cumulus merger, convective scale circulations, and the effects of cumulus downdrafts (Simpson, 1980; Simpson et al., 1980; Cunning and DeMaria, 1981; Cunning et al., 1982; Cooper et al., 1982; Holle and Maier, 1980; Purdom 1979) and their subsequent movement away from the originating storm into other regions can affect the development.

Finally, it can be summarily stated that the convection on any particular day over south Florida is the result of the interaction of many scales including the large, regional scale (Atlantic high pressure circulation), the synoptic scale (waves, fronts), the peninsular scale (sea and lake breezes), cloud scale (cumulus mergers, downdraft interaction), down to the local scale (surface feature variations such as soils and vegetation). Thus, it is probably beyond our current ability to understand completely the myriad factors and complex interactions that determine the exact convective pattern for any particular day. Bearing this limitation in mind, this paper has addressed the principal meteorological factors and types of flow patterns that differentiate between broad types of convective shower patterns. This approach has been successful in showing that there

is indeed a strong relationship between the observed convective patterns and the variations in the large scale flow.

6. ACKNOWLEDGMENTS

The completion of this study would not have been possible without the help and assistance of many people. I would like to thank Dr. William L. Woodley, former Program Manager of the Cumulus Dynamics and Microphysics Group, NOAA, for his enthusiasm and continuing support of this study.

Appreciation is also extended to Dr. Patrick T. Gannon, Sr. and Mr. Christopher C. Balch for providing the West Palm Beach and Miami, Florida atmospheric sounding information that played an important part in the analysis.

Thanks also are given to Mr. Andrew I. Watson for his help in implementing the objective analysis program, and in obtaining and extracting the radiosondé data that were used in the objective analysis.

I would also like to thank Drs. John A. Flueck and Paul W. Mielke for their many suggestions on methods to improve and consolidate the statistical presentation in this study. Without their guidance, the statistics would have overwhelmed anybody attempting to decipher them.

Finally, I would like to thank Mr. Ronald L. Holle, Dr. Roger A. Pielke, and Dr. Richard Johnson for all of their suggestions and encouraging words.

7. REFERENCES

Bellamy, J. C., 1949: Objective calculation of divergence, vertical velocity and vorticity. Bull. Am. Meteor. Soc., **30**, 45-49.

Burpee, R. W., 1979: Peninsula-scale convergence in the south Florida sea breeze. Mon. Wea. Rev., **107**, 852-860.

Burpee, R. W. and L. N. Lahiff, 1983: Peninsula-scale rainfall variations on sea-breeze days in south Florida. Submitted to Mon. Wea. Rev.

Byers, H. R. and H. R. Rodebush, 1948: Causes of thunderstorms of the Florida peninsula. J. Meteor., **5**, 275-280.

Carlson, T. N., 1967: Structure of a steady-state cold low. Mon. Wea. Rev., **95**, 763-777.

Cooper, H. J., M. Garstang, and J. Simpson, 1982: The diurnal interaction between convection and peninsular-scale forcing over south Florida. Mon. Wea. Rev., **110**, 486-503.

Cressman, G. P., 1958: An operational objective analysis system. Mon. Wea. Rev., **87**, 367-374.

Cumulus Group Staff, 1976: 1975 Florida Area Cumulus Experiment (FACE): Operational summary. NOAA Tech. Memo. ERL WMPO-28, U.S. Dept. of Commerce, Boulder, Colorado 80303, 186 pp.

Cumulus Group Staff, 1979: 1978 Florida Area Cumulus Experiment (FACE): Operation summary and data inventory. NOAA Tech. Memo. ERL NHEML-4, U.S. Dept. of Commerce, Boulder, Colorado 80303, 262 pp.

Cunning, J. B. and M. DeMaria, 1981: Comments on "Downdrafts as linkages in dynamic cumulus seeding effects". J. Appl. Meteor., **20**, 1081-1084.

Cunning, J. B., R. L. Holle, P. T. Gannon, Sr., and A. I. Watson, 1982: Convective evolution and merger in the FACE experimental area: Mesoscale convection and boundary layer interactions. J. Appl. Meteor., **21**, 953-977.

Day, S., 1953: Horizontal convergence and the occurrence of summer shower precipitation at Miami, Florida. Mon. Wea. Rev., **81**, 155-161.

Doneaud, A. A., P. L. Smith, A. S. Dennis, and S. Sengupta, 1981: A simple method for estimating rain volume over an area. Water Resour. Res., **17**, 1676-1682.

Estoque, M. A., 1962: The sea breeze as a function of the prevailing synoptic situation. J. Atmos. Sci., **19**, 244-250.

Frank, N. L., 1970: On the nature of upper tropospheric cold core cyclones over the tropical Atlantic. Ph.D. dissertation, The Florida State University, Tallahassee, 241 pp.

Frank, N. L., P. L. Moore, and G. E. Fisher, 1967: Summer shower distribution over the Florida peninsula as deduced from digitized radar data. J. Appl. Meteor., **6**, 309-316.

Frank, N. L. and D. L. Smith, 1968: On the correlation of radar echoes over Florida with various meteorological parameters. J. Appl. Meteor., **7**, 712-714.

Gannon, Sr., P. T., 1978: Influence of earth surface and cloud properties on the south Florida sea breeze. NOAA Tech. Rep. ERL 402 - NHEML 2. U.S. Dept. of Commerce, Boulder, Colorado 80303, 91 pp.

Gentry, R. C. and P. L. Moore, 1954: Relation of local and general wind interaction near the sea coast to time and location of air-mass showers. J. Meteor., **11**, 507-511.

Holle, R. L. and M. W. Maier, 1980: Tornado formation from downdraft interaction in the FACE mesonetwork. Mon. Wea. Rev., **108**, 1010-1027.

Holton, J. R., 1979: An Introduction to Dynamic Meteorology, 2nd ed., Academic Press, New York, New York 10003, 391 pp.

Jordan, C. L., 1957: Mean soundings for the West Indies area. J. Meteor., **15**, 91-97.

Kelly, W. E. and D. R. Mock, 1982: A diagnostic study of upper tropospheric cold lows over the western north Pacific. Mon. Wea. Rev., **110**, 471-480.

López, R. E., D. O. Blanchard, D. Rosenfeld, M. J. Casey, and W. L. Hiscox, 1981: FACE-2 data reductions and analysis (prior to disclosure of the treatment decisions): Part III, S- and C-band radar observations in support of FACE-2. NOAA Tech. Memo. ERL OWRM-7, U.S. Dept. of Commerce, Boulder, Colorado 80303, 267 pp.

López, R. E., D. O. Blanchard, D. Rosenfeld, W. L. Hiscox, and M. J. Casey, 1983a: Population characteristics, development processes, and structure of radar echoes in south Florida. Accepted for publication in Mon. Wea. Rev.

López, R. E., P. T. Gannon, Sr., D. O. Blanchard, and C. C. Balch, 1983b. Synoptic and regional circulation parameters associated with the degree of convective shower activity in south Florida. Accepted for publication in Mon. Wea. Rev.

López, R. E., J. Thomas, D. O. Blanchard, and R. L. Holle, 1983c: Estimation of rainfall over an extended region using only measurements of the area covered by radar echoes. Preprints, 21st Conference on Radar Meteorology, 681-686. American Meteorological Society, Boston, Mass.

McCumber, M. C., 1980: A numerical simulation of the influence of heat and moisture fluxes upon mesoscale circulations. Ph.D. dissertation, Dept. of Environmental Sciences, The University of Virginia, Charlottesville, 255 pp.

McPherson, R. D., 1970: A numerical study of the effect of a coastal irregularity on the sea breeze. J. Appl. Meteor., **9**, 767-777.

Mielke, P. W., K. J. Berry, and E. S. Johnson, 1976: Multi-response permutation procedures for a priori classifications. Communications in Statistics-Theory and Methods, **A5**, 1409-1424.

Mielke, P. W., K. J. Berry, and G. W. Brier, 1981: Application of multi-response permutation procedures for examining seasonal changes in monthly sea-level pressure patterns. Mon. Wea. Rev., **109**, 120-126.

Neumann, J. 1951: Land breezes and nocturnal thunderstorms. J. Meteor., **8**, 60-67.

Ostlund, S. S., 1974: Computer software for rainfall analysis and echo tracking of digitized radar data. NOAA Tech. Memo. ERL WMPO-15, U.S. Dept. of Commerce, Boulder, Colorado 80303, 82 pp.

Palmén, 1949: Origin and structure of high-level cyclones south of the maximum westerlies. Tellus, **1**, 22-31.

Pielke, R. A., 1973: An observational study of cumulus convective patterns in relation to the sea breeze over south Florida. NOAA Tech. Memo. ERL OD-16, U.S. Dept. of Commerce, Boulder, Colorado 80303, 81 pp.

Pielke, R. A., 1974: A three-dimensional numerical model of the sea breezes over south Florida. Mon. Wea. Rev., **102**, 115-139.

Pielke, R. A. and Y. Mahrer, 1978: Verification analysis of the University of Virginia three-dimensional mesoscale model prediction over south Florida for 1 July 1973. Mon. Wea. Rev., **106**, 1568-1589.

Purdom, J. F. W. 1979: The development and evolution of deep convection. Preprints, 11th Conference on Severe Local Storms, 143-150. American Meteorological Society, Boston, Mass.

Riehl, H., 1954: Tropical Meteorology. McGraw-Hill, 392 pp.

Riehl, H.. 1979: Climate and Weather in the Tropics. Academic Press, New York, New York 10003, 611 pp.

Simpson, J. S., 1980: Downdrafts as linkages in dynamic cumulus seeding effects. J. Appl. Meteor., **19**, 477-487.

Simpson, J. S., N. E. Wescott, R. J. Clerman, and R. A. Pielke, 1980: On cumulus mergers. Arch. Meteor. Geophys., Bioklimatol., Ser. A, **29**, 1-40.

Smith, D. L., 1970: The application of digitized radar data to the prediction of summertime convective activity in coastal regions. Preprints, 14th Radar Meteorology Conference, 347-352. American Meteorological Society, Boston, Mass.

Tukey, J. W., 1977: Exploratory Data Analysis, Addison-Wesely, Reading, Mass., 688 pp.

Wiggert, V. and G. F. Andrews, 1974: Digitizing, recording and computer processing weather radar data at the Experimental Meteorology Laboratory. NOAA Tech. Memo. ERL WMPO-17, U.S. Dept. of Commerce, Boulder, Colorado 80303, 70 pp.

Wiggert, V., S. S. Östlund, G. J. Lockett, and J. V. Stewart, 1976: Computer software for the assessment of growth histories of weather radar echoes. NOAA Tech. Memo. ERL WMPO-35, U.S. Dept. of Commerce, Boulder, Colorado 80303, 86 pp.

Wiggert, V. and G. J. Lockett, 1981: Radar rainshower growth histories and variations with wind speed, echo motion, location and merger status. Mon. Wea. Rev., **109**, 1467-1494.

Wood, R. W. and E. A. Fernald, 1974: The New Florida Atlas: Patterns of the Sunshine State. Rose Printing Company, Tallahassee, Florida.

Woodley, W. L., 1970: Precipitation results from a pyrotechnic cumulus seeding experiment. J. Appl. Meteor., **9**, 109-122.

Woodley, W. L., J. A. Jordan, J. S. Simpson, R. Biondini, J. A. Flueck, and A. G. Barnston, 1982: Rainfall results of the Florida Area Cumulus Experiment. J. Appl. Meteor., **21**, 139-164.